

Gamow-Teller transitions in some intermediate-mass nuclei

H. S. Wilson,* R. W. Kavanagh, and F. M. Mann†

W. K. Kellogg Radiation Laboratory, California Institute of Technology, Pasadena, California 91125

(Received 9 May 1980)

We present the results of an experimental study of allowed Gamow-Teller β^+ and electron-capture decays of ^{14}O , ^{21}Na , ^{25}Al , ^{26}Si , ^{29}P , ^{30}P , ^{30}S , ^{31}S , ^{33}Cl , ^{34}Cl , ^{35}Ar , ^{38}Ca , and ^{41}Sc . Thirteen new branches have been found and the precision has been increased, or upper limits reduced, on the intensities of more than 50 others.

$$\left[\begin{array}{l} \text{RADIOACTIVITY } ^{14}\text{O}, ^{21}\text{Na}, ^{25}\text{Al}, ^{26}\text{Si}, ^{29}\text{P}, ^{30}\text{P}, ^{30}\text{S}, ^{31}\text{S}, ^{33}\text{Cl}, ^{34}\text{Cl}^m, ^{35}\text{Ar}, \\ ^{38}\text{Ca}, ^{41}\text{Sc} \text{ measured } I_\gamma; ^{26}\text{Si}, ^{29}\text{P}, ^{30}\text{S}, ^{31}\text{S}, ^{34}\text{Cl}^m, ^{38}\text{Ca} \text{ measured } T_{1/2}. \end{array} \right]$$

I. INTRODUCTION

A stringent test of a nuclear structure calculation is the comparison of the measured strengths of β and γ transitions with the transition strengths derived from calculated wave functions. Moreover, because the parameters of the effective interaction in shell model calculations are frequently adjusted to obtain the best match between observed and calculated binding energies (e.g., Brown *et al.*¹ and Meurders *et al.*²) the comparison of transition rates is often the first independent test of the wave functions.

The connection between "allowed" β -decay rates, which are the concern of this paper, and the Fermi (F) and Gamow-Teller (GT) matrix elements connecting initial and final states is simple:

$$ft = \frac{6163.4 \pm 3.8 \text{ sec}}{|M_F|^2 + (g_A/g_V)^2 |M_{GT}|^2}. \quad (1)$$

The factor f is the phase-space factor determined by the total energy release, t is the half-life for the β decay from the initial to the final state, $6163.4 \pm 3.8 \text{ sec}$ is essentially the vector coupling constant determined by Hardy and Towner³ (Raman *et al.*⁴ recommend $6177.2 \pm 4.2 \text{ sec}$; the difference of 0.2% is negligible for our purposes), and $g_A/g_V = 1.250 \pm 0.009$ is the ratio of axial coupling constant to vector coupling constant.⁵ (A recent measurement of the half-life of the neutron⁶ would revise this value upward to 1.273 ± 0.005 ; we continue to use 1.250 ± 0.009 here.) The allowed approximation (nonrelativistic nucleons and long lepton wavelength) yields simple expressions for the matrix elements, $M_F = \langle \psi_f | \sum_j \tau_j^- | \psi_i \rangle$ and $M_{GT} = \langle \psi_f | \sum_j \tau_j^- \sigma_j | \psi_i \rangle$, and permits complete separation of the phase-space factor from the matrix elements.

Various estimates have shown that the error in the allowed approximations is quite small.

Barroso and Blin-Stoyle⁷ find that the relativistic correction for nuclei with a closed LS shell plus or minus one nucleon is a reduction of $\sim 2\%$ to 5% in the decay rate. Raman *et al.*⁸ calculated the effects on the phase-space factor f of higher-order terms in the lepton wave functions, and comparison with a less elaborate calculation, e.g., Gove and Martin,⁹ shows that these effects are less than 2% for positron end-point kinetic energies less than 6 MeV and for nuclei lighter than the calcium isotopes.

A further approximation in the connection between observed β -decay rates and nuclear structure is the assumption, implicit in most calculations and explicitly used in the expression above for M_{GT} , that the wave function can be expressed using only nucleon coordinates. In fact, strong interactions of the nucleons will result in the presence of non-nucleonic components in the nucleus (such as virtual Δ particles) which need not have the same GT decay properties as free nucleons, since the axial current is not conserved. The error introduced by this correction is probably not large; for closed LS -shell nuclei plus or minus one nucleon, Towner and Khanna¹⁰ have shown that the non-nucleonic components in the nuclear wave function change M_{GT} by $\lesssim 5\%$ (this number is, however, a sum of larger, canceling quantities).

Thus, the original expression connecting nuclear-structure calculations (which yield M_F and M_{GT}) to the experimental rates is presumably accurate to better than 10%. This is currently much less than the discrepancy between the results of model calculations and measurements.

The Fermi matrix element is the matrix element of the isospin-lowering operator. Studies of 0^+ , $T=1$ to 0^+ , $T=1$ β^+ decays^{3,4} have shown that isospin in low- and intermediate-mass nuclei is a good quantum number with deviations from pure isospin symmetry of $\lesssim 1\%$. Since nu-

clear structure calculations usually assume that states have pure isospin, there is no significance to comparisons of theory and experiment for Fermi transitions; the model has assumed the correct result from the beginning. Therefore, only Gamow-Teller transitions test such calculations. For mixed Fermi and Gamow-Teller transitions the GT component of a transition can be separated from the Fermi by using Eq. (1) and the well-known relation $M_F^2 = T(T+1) - T_3(T_3-1)$. (Wilkinson¹¹ prefers to reduce M_F^2 by the factor 0.995 ± 0.003 which assumes a small violation of isospin conservation.)

We report here a series of measurements of β^+ decay rates in intermediate-mass nuclei near the "valley of β stability" ($T=0$, $\frac{1}{2}$, or 1) and compare them to the results of several recent large-basis shell-model calculations.

II. EXPERIMENTAL PROCEDURES

Essentially the same program was followed for each of the thirteen positron decays reported here. A rabbit system (pneumatic shuttle) was used to transfer targets between a bombarding station, where the radioactivity was made using the p , d , ^3He , and α beams provided by the ONR-CIT tandem accelerator, and a well-shielded 100-cm³ Ge(Li) detector 10 to 20 m away. The beam passed through an exit foil of 25- μm Al or 2.5- μm Havar and a 2.4-mm-diam collimator before striking the target. At the detector, the rabbit stopped inside a block of Lucite or aluminum to trap the positrons. Transit times varied from 0.35 sec for the shortest half-lives to ~ 1 sec. The data acquisition, rabbit transfer, and beam blocking during periods when the target was not being bombarded were cycled by a crystal-controlled sequence timer. For the two long-lived activities studied, ^{30}P and $^{34}\text{Cl}^m$, the targets were carried by hand.

For each decay, the relative intensities of the daughter γ rays were determined from the Ge(Li) spectra. For the $T = \frac{1}{2}$ nuclei and for ^{30}P , absolute intensities were established by measuring the intensity of a strong γ ray relative to the intensity of the positron annihilation radiation. In three cases (^{26}Si , ^{30}S , and ^{38}Ca), absolute normalization was made by measuring the half-life precisely and comparing it to the calculated half-life for the 0^+ to 0^+ superallowed Fermi branch in the decay. The details of the three procedures are given in order below, along with a brief discussion of calculated uncertainties in weighted averages.

A. Relative γ -ray intensities

In cases where only the intensities of weak, high-energy γ rays relative to intense lower-

energy γ rays were sought, Pb absorbers ranging from 1.3 to 4.4 cm thick were used to reduce the count rate due to annihilation radiation. In two cases ($^{34}\text{Cl}^m$ and ^{38}Ca) runs were also made with no Pb in order to measure the intensities of 146- and 328-keV γ rays, respectively. Ge(Li) spectra were recorded in two sequential 4096-channel groups, each group lasting about a half-life of the radioactivity being studied in order to permit a rough determination of half-life for observed γ rays.

Relative-efficiency calibrations were performed using the following radioactive sources: ^{56}Co and ^{66}Ga (Refs. 12 and 13), ^{182}Ta (Ref. 14), and ^{207}Bi (Refs. 15-17). In addition, calibrated ^{133}Ba , ^{137}Cs , ^{60}Co , and ^{22}Na sources were used to connect the 300-keV region of the spectrum to the region spanned by ^{56}Co and ^{66}Ga . For these sources γ -ray intensities were taken from Refs. 18-21. The $^{14}\text{N}(p,\gamma)^{15}\text{O}$ resonant capture reaction²² at $E_p = 1.058$ MeV was used to extend the relative-efficiency calibration to 5.24 and 8.28 MeV, with the detector set up at the bombardment station.

Corrections for the effect of two (or more) photons summing in the detector were made to all calibration and experimental spectra. A computer program which took into account detector size and shape and absorbers was used to calculate absolute total efficiencies. These calculations (which did not include the effects of Compton scattering in the materials around the detector) were then multiplied by a factor to reproduce the efficiencies measured at 661, 1173, and 1333 keV using calibrated ^{137}Cs and ^{60}Co sources. The validity of this approach (using an energy-independent factor) is demonstrated by the fact that the factor determined for the 661-keV efficiency was within 10% of the factor for the higher-energy γ rays. The photon-attenuation coefficients given by Grodstein²³ were used to take into account small differences between the calibration and the experimental geometries. The only large corrections made were to adapt $^{14}\text{N}(p,\gamma)^{15}\text{O}$ relative-efficiency calibrations made with 2.5 cm of Pb absorber to geometries with 3.2 and 4.4 cm of Pb.

B. Absolute γ -ray intensities

As mentioned previously, the absolute γ -ray intensities (i. e., number of γ rays per decay) were measured by comparing the intensities of γ rays to the intensity of the 511-keV radiation produced by the annihilation of stopped positrons from the same decay. Blocks of Lucite or aluminum ("hutches") surrounding the rabbit at the detector and of the rabbit system trapped the positrons with a minimum of bremsstrahlung. For these

measurements, only 0.64 cm of Pb absorber or else no Pb were used to avoid excessive absorption and scattering of 511-keV photons (except for the 2796-keV γ ray in ^{21}Na). In these cases data were recorded in 4, 8, or 16 consecutive spectra, partitioning the 8192 available channels. A constant-rate pulser peak in the spectrum allowed a correction to be made to peak areas to account for pulse pileup and analyzer dead-time losses. The multispectral scaling permitted the use of a computer program to separate the area of the 511-keV peak into components with half-lives specified in the program's input. From this the ratio [area (γ ray)/area (511 due to activity being studied)] was calculated. A computer program calculated the effects of the distributed source of the 511-keV radiation, absorption of 511-keV radiation in the rabbit, and in-flight annihilation of the positrons on the efficiency for detecting a count in the 511-keV photopeak when a positron is emitted. The in-flight annihilation was calculated using the formulas for one- and two-quantum annihilation given by Azuelos and Kitching.²⁴ The positron stopping powers of the various materials in the target and rabbit system were calculated following Nelms²⁵ but including small density-effect corrections given by Sternheimer²⁶ and also the radiative stopping power calculated using formula $3BN$ given by Koch and Motz²⁷ for bremsstrahlung production.

It was found that the effect of the distributed source was very small in our geometry. The in-flight-annihilation probability ranged from 0.8% for ^{22}Na positrons to 7.5% for ^{41}Sc positrons. We also estimated that the "reflection" of positrons from Pb and Ta target backings changed the efficiencies for detecting 511-keV radiation by $\sim 6\%$.

A ^{22}Na source was counted in a geometry as similar as possible to the experimental case (in most cases, the ^{22}Na source was prepared by evaporating $^{22}\text{NaCl}$ solution in a rabbit identical to the ones used in the experiment). We used 0.1060 ± 0.0017 for the electron capture to positron ratio in ^{22}Na decay.²⁸ Calibration using ^{56}Co sources (and calibrated ^{133}Ba , ^{60}Co , and ^{22}Na sources in the ^{21}Na experiment) gave the detection efficiency for the γ ray being studied relative to the 1275-keV γ ray from ^{22}Na . Summing corrections were applied to all spectra as described earlier and a small correction was made for the contribution to the 511-keV peak from electron-positron pairs produced in the Pb shields around the detector by high-energy γ rays and in-flight-annihilation photons. The result of these calculations is the efficiency for detecting the γ ray relative to the efficiency for detecting the positrons (i. e., 511-keV annihilation photons). Combined

with the peak-area ratio, this gives the absolute intensity of the γ ray.

C. Half-life measurements

For these experiments, data were collected in 8 or 16 consecutive spectra, each lasting 0.3 to 0.5 half-lives. The half-life was then determined by fitting the areas of a strong γ ray with a simple exponential. A "leaky integrator" ensured that the same amount of the radioactivity of interest was produced on each cycle and a constant-rate pulser was fed into the Ge(Li) preamp in order to monitor peak losses due to analyzer dead time and pulse pileup. The computed fit to the peak areas took account of the fact that, since the group dwell time was comparable to the half-life of the radioactivity, the count-rate-dependent losses could change substantially during a single group and, as a result, the losses from a γ -ray peak originating in a short-lived activity were significantly greater than the losses from the pulser peak.

The half-lives of ^{29}P and ^{31}S were also measured, but by following the decay of the 511-keV peak, since these activities have no intense γ ray. These data were analyzed as described previously, separating the 511-keV peak areas into components with specified half-lives as input and calculating a value of χ^2 for the fit. Thus, the minimum of χ^2 as a function of the half-life of the activity being studied determined a best value, with the uncertainty defined by the points $\chi_{\min}^2 + 1$, which lie one standard deviation above and below the mean [here we use a likelihood distribution $\mathcal{L} \sim \exp(-\chi^2/2)$].

D. Uncertainties in weighted averages

Frequently the scatter among several independent measurements was significantly greater than it should have been by chance, as determined by the χ^2 criterion. For a set of N measurements $x_i \pm \sigma_i$, the statistical uncertainty on the weighted average is $\sigma = [\sum_{i=1}^N (1/\sigma_i^2)]^{-1/2}$. Generally, in those cases where the value of χ^2 obtained was so large that the probability of a larger value occurring by chance was less than 25%, the statistical uncertainty on the weighted average was multiplied by $(\chi^2/\chi_0^2)^{1/2}$, where χ_0^2 is the 50% point of the χ^2 distribution for $N-1$ degrees of freedom. For smaller values of χ^2 , the simple statistical uncertainty on the weighted average is given.

III. EXPERIMENTAL RESULTS

In this section we present the results of our measurements and additional details of experimental procedures. Table I lists the absolute β branches derived from our work and compares

TABLE I. Absolute β -branch intensities and Gamow-Teller $\log ft$ values.

Decay (half-life) ^b	Final state ^a		Absolute branch intensity (%)		$\log ft$ (exp) ^c
	E_x (keV)	J^π	This work	Previous ^a	
$^{14}\text{O}(0^+) \rightarrow ^{14}\text{N}$ (70.599 \pm 0.058 sec)	0	1 ⁺	0.61 \pm 0.01 ^a	0.61 \pm 0.01	7.266 \pm 0.009
	2313	0 ⁺	99.332 \pm 0.011	99.328 \pm 0.012	
	3948	1 ⁺	0.0577 \pm 0.0043	0.063 \pm 0.007	3.112 \pm 0.034
$^{21}\text{Na}(\frac{3}{2}^+) \rightarrow ^{21}\text{Ne}$ (22.48 \pm 0.03 sec)	0	$\frac{3}{2}^+$	94.98 \pm 0.13	94.9 \pm 0.2	3.614 \pm 0.007 4.092 \pm 0.021 (GT)
	351	$\frac{5}{2}^+$	5.02 \pm 0.13 ^d	5.1 \pm 0.2	4.605 \pm 0.014
	2796	$\frac{1}{2}^+$	(3.98 \pm 0.75) $\times 10^{-4}$		4.62 \pm 0.09
$^{26}\text{Si}(0^+) \rightarrow ^{26}\text{Al}$ (2.2345 \pm 0.0090 sec)	228	0 ⁺	75.03 \pm 0.46 ^e	74.9 \pm 0.9	
	1058	1 ⁺	21.89 \pm 0.41	21.8 \pm 0.9	3.550 \pm 0.011
	1850	1 ⁺	2.726 \pm 0.070	2.9 \pm 0.2	3.855 \pm 0.013
	2072	1 ⁺	0.290 \pm 0.011	0.4 \pm 0.1	4.629 \pm 0.018
	2739	1 ⁺	0.0618 \pm 0.0025		4.539 \pm 0.019
	3723	1 ⁺	<0.0013		>4.15
$^{29}\text{P}(\frac{1}{2}^+) \rightarrow ^{29}\text{Si}$ (4.117 \pm 0.038 sec)	0	$\frac{1}{2}^+$	98.291 \pm 0.031	98.8 \pm 0.2	3.686 \pm 0.008 4.360 \pm 0.038 (GT)
	1273	$\frac{3}{2}^+$	1.255 \pm 0.022	1.1 \pm 0.2	4.814 \pm 0.011
	2028	$\frac{5}{2}^+$	<0.0048	<0.07	>6.59
	2426	$\frac{3}{2}^+$	0.456 \pm 0.014	0.10 \pm 0.07	4.178 \pm 0.016
$^{30}\text{P}(1^+) \rightarrow ^{30}\text{Si}$ (149.88 \pm 0.24 sec)	0	0 ⁺	99.9397 \pm 0.0028	99.931 \pm 0.012	4.839 \pm 0.007
	2235	2 ⁺	0.0551 \pm 0.0026 ^f	0.069 \pm 0.012	5.879 \pm 0.023
	3499	2 ⁺	(1.56 \pm 0.15) $\times 10^{-3}$		5.253 \pm 0.044
	3770	1 ⁺	(1.83 \pm 0.36) $\times 10^{-4}$		5.787 \pm 0.088
	3788	0 ⁺	(3.39 \pm 0.29) $\times 10^{-3}$		4.476 \pm 0.039
$^{30}\text{S}(0^+) \rightarrow ^{30}\text{P}$ (1.1786 \pm 0.0045 sec)	0	1 ⁺	21.31 \pm 0.46	19.4 \pm 1.0	4.327 \pm 0.012
	677	0 ⁺	76.11 \pm 0.44 ^g	77.5 \pm 1.0	
	709	1 ⁺	0.293 \pm 0.069	0.5 \pm 0.2	5.91 \pm 0.11
	3019	1 ⁺	2.283 \pm 0.054	2.60 \pm 0.17	3.562 \pm 0.012
	3304	(0 ⁺ , 1 ⁺)	<0.075		>4.76
	3731	1 ⁺	<0.011		>5.10
	3927	(1 ⁺ , 2 ⁻ , 3 ⁺)	<0.074		>4.01
	4235		<0.048		>3.67
	4343	π =unnat.	<0.021		>3.81
	4501	1 ⁺	<0.0073		>3.92

TABLE I. (Continued).

Decay (half life) ^b	Final state ^a		Absolute branch intensity (%)		logft (exp)
	E_x (keV)	J^π	This work	Previous ^a	
$^{31}\text{S}(\frac{1}{2}^+) \rightarrow ^{31}\text{P}$ (2.562 ± 0.012 sec)	0	$\frac{1}{2}^+$	98.86 ± 0.04	98.75 ± 0.05	3.682 ± 0.007 4.341 ± 0.003 (GT)
	1266	$\frac{3}{2}^+$	1.097 ± 0.033 ^h	1.20 ± 0.06	4.966 ± 0.015
	3134	$\frac{1}{2}^+$	0.0326 ± 0.0016	0.034 ± 0.005	4.770 ± 0.023
	3506	$\frac{3}{2}^+$	0.0121 ± 0.0010	0.012 ± 0.004	4.538 ± 0.038
	4261	$\frac{3}{2}^+$	<2.8 × 10 ⁻⁴		>4.71
	4594	$\frac{3}{2}^+$	<2.5 × 10 ⁻⁴		>4.45
$^{33}\text{Cl}(\frac{3}{2}^+) \rightarrow ^{33}\text{S}$ (2.511 ± 0.004 sec) ⁱ	0	$\frac{3}{2}^+$	98.58 ± 0.19	98.3 ± 0.2	3.755 ± 0.007 4.88 ± 0.10 (GT)
	841	$\frac{1}{2}^+$	0.479 ± 0.064	0.54 ± 0.10	5.666 ± 0.059
	1966	$\frac{5}{2}^+$	0.460 ± 0.060 ^j	0.56 ± 0.06	4.982 ± 0.058
	2312	$\frac{3}{2}^+$	0.0353 ± 0.0048	<0.05 ^k	5.828 ± 0.060
	2866	$\frac{5}{2}^+$	0.443 ± 0.058 ^j	0.56 ± 0.06	4.194 ± 0.058
	3832	$\frac{5}{2}^+$	<9.2 × 10 ⁻⁴		>5.40
	3935	$\frac{3}{2}^+$	<7.0 × 10 ⁻⁴		>5.30
	4053	$\frac{1}{2}^+$	(4.7 ± 1.5) × 10 ⁻⁴		5.24 ± 0.15
	4144	$(\frac{3}{2}^+, \frac{5}{2}^+)$	<2.6 × 10 ⁻⁴		>5.28
	4375	$\frac{1}{2}^+$	<4.4 × 10 ⁻⁴		>4.65
	4424	$(\frac{1}{2}^+, \frac{3}{2}^+)$	<5.7 × 10 ⁻⁴		>4.49
	4746		(4.1 ± 1.2) × 10 ⁻⁴		4.37 ± 0.14
	$^{34}\text{Cl}(0^+) \rightarrow ^{34}\text{S}$ (1.5262 ± 0.0025 sec)	0	0 ⁺	100	
4072		1 ⁺	<0.00078	<0.0022 ^l	>4.53
$^{34}\text{Cl}^m(3^+) \rightarrow ^{34}\text{S}$ (32.01 ± 0.04 min) ⁱ	2127	2 ⁺	28.53 ± 0.52	28.4 ± 0.7	5.994 ± 0.010
	3303	2 ⁺	26.42 ± 0.29	24.3 ± 0.7	4.831 ± 0.008
	4114	2 ⁺	0.458 ± 0.010	0.392 ± 0.015	5.089 ± 0.012
	4688	4 ⁺	0.0336 ± 0.0029	0.030 ± 0.006	5.431 ± 0.039
	4876	3 ⁺	0.0382 ± 0.0060	0.032 ± 0.003	5.190 ± 0.071
	4889	2 ⁺	<0.0013	<0.00087 ^l	>6.64
$^{35}\text{Ar}(\frac{3}{2}^+) \rightarrow ^{35}\text{Cl}$ (1.773 ± 0.003 sec) ⁱ	0	$\frac{3}{2}^+$	98.235 ± 0.052	98.28 ± 0.05 ^m	3.760 ± 0.06 4.95 ± 0.10 (GT)
	1219	$\frac{1}{2}^+$	1.228 ± 0.034 ^h	1.22 ± 0.05	5.100 ± 0.014
	1763	$\frac{5}{2}^+$	0.272 ± 0.010	0.229 ± 0.011	5.444 ± 0.017
	2694	$\frac{3}{2}^+$	0.1606 ± 0.0065	0.19 ± 0.02	5.006 ± 0.019
	3003	$\frac{5}{2}^+$	0.0901 ± 0.0033	0.08 ± 0.02	4.975 ± 0.017
	3918	$\frac{3}{2}^+$	(7.90 ± 0.52) × 10 ⁻³		4.880 ± 0.030
	3968	$\frac{1}{2}^+$	(7.44 ± 0.87) × 10 ⁻³		4.825 ± 0.053
	4624	$(\frac{3}{2}^+, \frac{5}{2}^+)$	<4.4 × 10 ⁻⁴		>4.75

TABLE I. (Continued).

Decay (half life) ^b	Final state ^a		Absolute branch intensity (%)		logft (exp) ^c
	E_x (keV)	J^π	This work	Previous ^a	
$^{38}\text{Ca}(0^+) \rightarrow ^{38}\text{K}$ (0.435 ± 0.009 sec)	130	0 ⁺	76.1 ± 1.7 ⁿ	75 ± 2	
	459	1 ⁺	2.66 ± 0.35	<3	4.827 ± 0.062
	1698	1 ⁺	21.0 ± 1.6	24 ± 2	3.398 ± 0.038
	3316	(1 ⁺ , 2 ⁻ , 3 ⁺)	<0.13		>4.58
	3342	1 ⁺	0.291 ± 0.038	(0.6 ± 0.2)	4.227 ± 0.060
	3702	(0 ⁺ -4 ⁺)	<0.25		>3.97
	3739	(1 ⁺ -5 ⁺)	<0.075		>4.46
	3841	$\pi = \text{unnat.}$	<0.10		>4.24
	3857	1 ⁺	<0.075		>4.34
	3978	1 ⁺	<0.23		>3.74
	4214	(0 ⁺ -2 ⁺)	<0.086		>3.89
	4318	(1 ⁺ -5 ⁺)	<0.040		>4.09
	4395	(1 ⁺ -5 ⁺)	<0.078		>3.70
$^{41}\text{Sc}(\frac{7}{2}^-) \rightarrow ^{41}\text{Ca}$ (0.5963 ± 0.0017 sec)	0	$\frac{7}{2}^-$	99.963 ± 0.003	100 ^o	3.461 ± 0.007 3.736 ± 0.014 (GT)
	2575	$\frac{5}{2}^-$	(2.32 ± 0.29) × 10 ⁻²	<0.2 ^o	5.82 ± 0.06
	2959	$\frac{7}{2}^-$	(1.39 ± 0.14) × 10 ⁻²	<0.2 ^o	5.77 ± 0.05
	3676	$\frac{3}{2}^-$	<3.4 × 10 ⁻³		>5.75
	4342	$\frac{3}{2}^-$	<1.0 × 10 ⁻³		>5.45
	4878	$\frac{5}{2}^-$	<1.1 × 10 ⁻³		>4.49
	5355	$\frac{7}{2}^-$	<7.9 × 10 ⁻⁴		>4.01
	5646	$\frac{7}{2}^-, \frac{5}{2}^-$	<1.1 × 10 ⁻³		>3.61
	5796	$\frac{7}{2}^-, \frac{5}{2}^-$	<1.2 × 10 ⁻³		>3.41

^aReferences 28 and 29, except where noted.

^bHalf-lives from Ref. 28 and Table III of this paper, except where noted.

^cBased on our β branches only. Logf values are taken from Ref. 9 with radiative corrections following Ref. 3.

^dWeighted average of this work and Ref. 33.

^eBased on assumed partial half-life of 2.978 ± 0.014 sec for the superallowed Fermi branch.

^fWeighted average of this work and Ref. 44.

^gBased on assumed partial half-life of 1.5485 ± 0.0067 sec for the superallowed Fermi branch.

^hWeighted average of this work and several previous results. See text.

ⁱSee text.

^jWeighted average of this work and Ref. 37.

^kReference 37.

^lReference 56. As described in the text, small corrections have been applied to the values reported by Ref. 56.

^mReference 86.

ⁿBased on assumed partial half-life of 0.5716 ± 0.0048 for the superallowed Fermi branch.

^oReference 71. The sum of the β^+ branch intensities to states above 3 MeV is <0.02%.

with previous work. Simple weighted averages between the results of this work reported in Table I and previous work should not be taken, since the absolute intensities of the strong γ rays, used to normalize our relative γ -ray intensities, are usually weighted averages with previous work (as are also the half-lives of ^{26}Si , ^{29}P , ^{30}S , ^{31}S ,

$^{34}\text{Cl}^m$, and ^{38}Ca). Rather, the average of this work and previous work should be calculated by averaging relative γ -ray intensities, half-lives, and absolute γ -ray intensities separately and then determining absolute β -branch intensities and logft values.

In Table I, logft values are calculated from the

tables of Gove and Martin⁹ and radiative corrections are applied following Hardy and Towner.³ Where necessary, γ branching ratios have been taken from the compilations of Ajzenberg-Selove²⁹ and Endt and Van der Leun,²⁸ to whom we also refer the reader for level diagrams and a summary of experimental results prior to 1978.

For each decay we also present separately the measured relative γ -ray intensities (except for ²⁵Al) and the measurements of the absolute intensity of the strongest γ rays and half-lives.

The comparison between our results for $\log ft$ values and large-basis shell-model calculations is made in Table II. Where authors have used axial and vector coupling constants other than the ones given earlier (i. e., $g_A/g_V = 1.250 \pm 0.009$ and $ft = 6163.4 \pm 3.8$ sec for pure Fermi transitions with $|M_F|^2 = 1$), we have recalculated their results with these coupling constants.

All limits given here are at the 2σ level (98% confidence). Table III summarizes the results of our half-life measurements and previously reported results.

A. ¹⁴O decay

The Gamow-Teller branch to the ground state of ¹⁴N is the mirror of the famous allowed, but highly hindered, β^- decay of ¹⁴C and has²⁹ $\log ft = 7.266 \pm 0.009$. The only other energy-allowed Gamow-Teller transition in this decay is to the 3948-keV level which decays principally to the 2313-keV level emitting a 1635-keV γ ray.

In this experiment, the ¹⁴O activity was made by the reaction ¹⁴N(p, n)¹⁴O using 11.0-MeV protons on targets of NH₄Cl powder wrapped in 25- μ m Ta foil and mounted in Be rabbits. The 1.8-sec ³⁵Ar activity in the target decayed during a 10-sec wait between the time the beam was blocked and the start of the counting period. Data were accumulated in two consecutive spectra, each lasting 70 sec. A 3.2-cm Pb absorber reduced the detector's absolute total efficiency for 511-keV annihilation radiation to $\sim 2 \times 10^{-4}$.

Figure 1 shows a typical spectrum from this experiment and Fig. 2 is a detailed plot of the region near 1635 keV. The presence of the Compton edge of the single-escape peak from the intense 2313-keV γ ray complicated the background subtraction; the solid lines in Fig. 2 are four-parameter least-squares fits in which the background is described as a quadratic plus a fraction of the Compton edge of the 511-keV peak in the same spectrum.

Taken with the ground-state β^+ branch²⁹ in ¹⁴O, (0.61 \pm 0.01)%, these measurements indicate that the intensity of the branch to the 3948-keV level in ¹⁴N is $(5.77 \pm 0.43) \times 10^{-20}\%$ with $\log ft = 3.112 \pm$

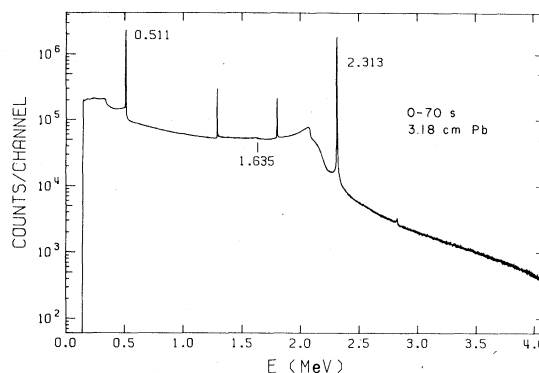


FIG. 1. One of three similar Ge(Li) spectra taken in the ¹⁴O experiment. The energy calibration is 0.9988 keV/channel.

0.034, in agreement with the previous value $(6.2 \pm 0.7) \times 10^{-20}\%$, reported by Kavanagh and Knipper.³⁰ Table II compares this result with the calculations of Cohen and Kurath³¹ and of Hauge and Maripuu.³²

B. ²¹Na decay

²¹Na activity was made by the reaction ²⁴Mg(p, α)²¹Na in rabbits of solid natural magnesium using 12- and 13-MeV protons. Following bombardment, a delay of more than 50 sec allowed the intense ²⁵Al and ²⁶Al activity, also produced in the targets, to decay before the start of counting. Data were collected in 16 consecutive groups of 20.0 sec for runs 1 and 2 and in 16 groups of 12.0 sec for runs 3 and 4. No Pb absorber was used. The first two runs established that, at the start of the counting period, more than 95% of the annihilation radiation was due to ²¹Na decay and $\sim 3\%$ was due to ²⁵Al and ²⁶Al. Areas of the 351-keV peak were calculated with allowance for curvature in the background in this region of the

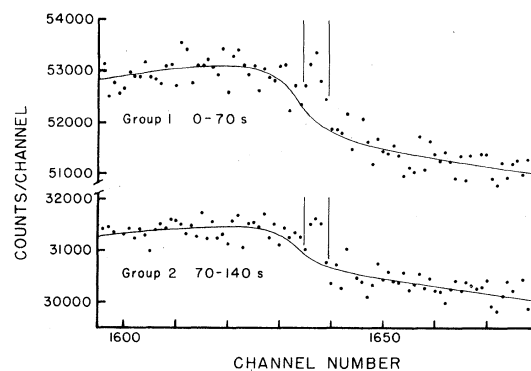


FIG. 2. Detailed plot of the spectrum near 1635 keV. The group 1 data (0-70 sec) are the data shown in Fig. 1. The vertical lines indicate channels included in calculating the peak area.

TABLE II. Comparison of measured Gamow-Teller $\log ft$ values and shell-model calculations.

Decay	Final state ^a		$\log ft$ (exp) ^b (GT part only)	$\log ft$ (theory) (GT part only)		
	E_x (keV)	$J^\pi; T$		c	d	
¹⁴ O(0 ⁺) → ¹⁴ N	0	1 ⁺	7.266 ± 0.009	4.92	4.32	
	3948	1 ⁺	3.112 ± 0.034	2.94	3.00	
²¹ Na($\frac{3}{2}^+$) → ²¹ Ne	0	$\frac{3}{2}^+$	4.092 ± 0.021	3.89	3.92	
	351	$\frac{5}{2}^+$	4.605 ± 0.014	4.36	4.52	
	2796	$\frac{1}{2}^+$	4.62 ± 0.07	4.95	4.32	
²⁶ Si(0 ⁺) → ²⁶ Al	1058	1 ⁺	3.550 ± 0.011	3.37	3.46 ± 0.11	
	1858	1 ⁺	3.855 ± 0.013	3.87	3.57 ± 0.17	
	2072	1 ⁺	4.629 ± 0.018	3.80	4.2	
	2739	1 ⁺	4.539 ± 0.019	4.29		
	3723	1 ⁺	>4.15			
²⁸ P($\frac{1}{2}^+$) → ²⁸ Si	0	$\frac{1}{2}^+$	4.360 ± 0.038	4.50	4.05	
	1273	$\frac{3}{2}^+$	4.814 ± 0.011		4.64	
	2426	$\frac{3}{2}^+$	4.178 ± 0.016		4.05	
³⁰ P(1 ⁺) → ³⁰ Si	0	0 ⁺	4.839 ± 0.007	5.53	3.82	3.82
	2235	2 ⁺	5.879 ± 0.023	4.83	4.59	4.89
	3499	2 ⁺	5.253 ± 0.044		4.34	
	3770	1 ⁺	5.79 ± 0.09		5.09	
	3788	0 ⁺	4.476 ± 0.039		4.51	
³⁰ S(0 ⁺) → ³⁰ P	0	1 ⁺	4.327 ± 0.012	5.06	3.34	3.34
	709	1 ⁺	5.91 ± 0.11	4.54	5.32	4.85
	3019	1 ⁺	3.562 ± 0.012	3.95	4.23	
	3731	1 ⁺	>5.10			
	4501	1 ⁺ ; 1	>3.92		4.62	
³¹ S($\frac{1}{2}^+$) → ³¹ P	0	$\frac{1}{2}^+$	4.341 ± 0.033	4.32	3.69	3.70
	1266	$\frac{3}{2}^+$	4.966 ± 0.015	4.97	4.77	4.72
	3134	$\frac{1}{2}^+$	4.770 ± 0.023	4.47	4.10	
	3506	$\frac{3}{2}^+$	4.538 ± 0.038	4.03	4.55	
	4261	$\frac{3}{2}^+$	>4.71			
	4594	$\frac{3}{2}^+$	>4.45			

TABLE II. (Continued).

Decay	Final state ^a		log <i>ft</i> (exp) ^b (GT part only)	log <i>ft</i> (theory) (GT part only)			
	<i>E_x</i> (keV)	<i>J^π</i> ; <i>T</i>		e	f	h	
³³ Cl($\frac{3}{2}^+$) → ³³ S	0	$\frac{3}{2}^+$	4.88 ± 0.10	5.06	4.17	4.15	
	841	$\frac{1}{2}^+$	5.666 ± 0.059	5.17	4.92	5.13	
	1966	$\frac{5}{2}^+$	4.982 ± 0.058	7.19	4.27		
	2312	$\frac{3}{2}^+$	5.828 ± 0.060	4.90	4.88		
	2866	$\frac{5}{2}^+$	4.194 ± 0.058	3.88	4.33		
	3832	$\frac{5}{2}^+$	> 5.40				
	3935	$\frac{3}{2}^+$	> 5.30				
	4053	$\frac{1}{2}^+$	5.24 ± 0.15				
	4144	($\frac{3}{2}^+$, $\frac{5}{2}^+$)	> 5.28				
	4375	$\frac{1}{2}^+$	> 4.65				
	4424	($\frac{1}{2}^+$, $\frac{3}{2}^+$)	> 4.49				
4746		4.37 ± 0.14					
³⁴ Cl(0 ⁺) → ³⁴ S	4072	1 ⁺ ; 1	> 4.53	4.44			
³⁴ Cl(3^+) → ³⁴ S	2127	2 ⁺	5.994 ± 0.010	7.53	5.86	7.13	
	3303	2 ⁺	4.831 ± 0.008	4.77	4.24	4.36	
	4114	2 ⁺	5.089 ± 0.012	4.71	8.12	5.15	
	4688	4 ⁺	5.431 ± 0.039	5.49	6.46		
	4876	3 ⁺	5.190 ± 0.071	4.76	4.91		
	4889	2 ⁺	> 6.64	4.99			
³⁵ Ar($\frac{3}{2}^+$) → ³⁵ Cl	0	$\frac{3}{2}^+$	4.95 ± 0.10	4.71	4.73 ± 0.05		
	1219	$\frac{1}{2}^+$	5.100 ± 0.014	4.83	4.47		
	1763	$\frac{5}{2}^+$	5.444 ± 0.017	7.91	5.82		
	2694	$\frac{3}{2}^+$	5.006 ± 0.019	4.66	4.27		
	3003	$\frac{5}{2}^+$	4.975 ± 0.017	4.35	4.14		
	3918	$\frac{3}{2}^+$	4.880 ± 0.030		4.53		
	3968	$\frac{1}{2}^+$	4.825 ± 0.053				
	4624	($\frac{3}{2}^+$, $\frac{5}{2}^+$)	> 4.75				
³⁸ Ca(0 ⁺) → ³⁸ K	459	1 ⁺	4.827 ± 0.062	3.85	6.18	3.85	5.58
	1698	1 ⁺	3.398 ± 0.038	3.07	3.03	4.44	3.25
	3342	1 ⁺	4.227 ± 0.060	3.97			
	3857	1 ⁺	> 4.34				
	3978	1 ⁺	> 3.74				

TABLE II. (Continued).

Decay	Final state ^a		log <i>ft</i> (exp) ^b (GT part only)	log <i>ft</i> (theory) (GT part only)
	<i>E_x</i> (keV)	<i>J^π</i> ; <i>T</i>		
⁴¹ Sc($\frac{7-}{2}$) → ⁴¹ Ca	0	$\frac{7-}{2}$	3.736 ± 0.014	k
	2575	$\frac{5-}{2}$	5.82 ± 0.06	5.58
	2959	$\frac{7-}{2}$	5.77 ± 0.05	5.64
	3676	$\frac{9-}{2}$	>5.75	
	4342	$\frac{9-}{2}$	>5.45	
	4878	$\frac{5-}{2}$	>4.49	4.42
	5355	$\frac{7-}{2}$	>4.01	
	5646	$\frac{7-}{2}, \frac{5-}{2}$	>3.61	4.06
	5796	$\frac{7-}{2}, \frac{5-}{2}$	>3.41	4.42

^aReference 28.^bSee Table I.^cReference 31.^dReference 32.^eReference 1.^fReference 74.^gReference 73.^hReference 75.ⁱReference 72.^jReference 76.^kCalculated from spectroscopic factors in Ref. 28. We assume that the 5646- and 5796-keV levels are $\frac{5-}{2}$.

Ge(Li) spectrum due to the Compton edge of the 511-keV peak. The efficiency calibration was made using calibrated ¹³³Ba, ⁶⁰Co, and ²²Na sources, and a ²²Na source prepared by evaporating a few drops of ²²NaCl solution in one of the rabbits. The small corrections discussed earlier were made, the most important one being (3.9 ± 0.2)% due to in-flight-annihilation loss for ²¹Na positrons compared to (0.8 ± 0.1)% for ²²Na. The total uncertainty in the efficiency calibration was ± 3.0%. The four runs were not in good agreement, giving branches to the 351-keV level in ²¹Ne (in percent) of 5.126 ± 0.091, 4.999 ± 0.080, 4.883 ± 0.071, and 4.930 ± 0.074 (the common error due to uncertainty in the efficiency calibration has not been included). The weighted average of the four numbers is 4.968 ± 0.056. Including the 3.0% uncertainty in the efficiency calibration gives our final result of (4.97 ± 0.16)% for the branch of the 351-keV level. This agrees with the value reported by Alburger³³ (5.1 ± 0.2)%, but disagrees with Azuelos *et al.*³⁴ who obtained (4.2 ± 0.2)%.

In a second experiment, a search was made for an electron-capture transition to the $\frac{1}{2}^+$ level at 2796 keV in ²¹Ne. The same targets were used as in the first experiment; the beam energy was raised to 13 MeV, and a 3.2-cm Pb γ -ray ab-

sorber was inserted. Data were recorded in four consecutive spectra of 15 sec each in order to separate the ²¹Na component of the annihilation radiation from the ²⁵Al and ²⁶Al^m. Pileup rejection was used to reduce the background in the high-energy part of the spectrum; spectra taken in coincidence with the signal indicating a pileup event showed that (0.4 ± 0.1)% of the 511-keV counts were falsely rejected and that above 1 MeV no peak was present in the rejected spectrum. Relative efficiencies were measured with ²²Na and ⁵⁶Co sources. Spectra collected in this experiment are displayed in Figs. 3 and 4. Taking into account the small corrections discussed earlier, we obtain an intensity of (3.98 ± 0.75) × 10⁻⁴% for the 2796-keV γ ray.

C. ²⁵Al decay

This decay has been studied previously in this laboratory.³⁵ At that time only the relative intensities of the γ rays were measured and normalization was based on a previously published value for the absolute intensity of the 1612-keV γ ray. We report here a new measurement of the 1612-keV intensity.

Targets were prepared by evaporating ²⁴Mg metal (enriched to 99.96% ²⁴Mg) onto 0.25-mm-

TABLE III. Half-life measurements.

$^{26}\text{Si} \rightarrow ^{26}\text{Al}$ (sec)	$^{29}\text{P} \rightarrow ^{29}\text{Si}$ (sec)	$^{30}\text{S} \rightarrow ^{30}\text{P}$ (sec)	$^{31}\text{S} \rightarrow ^{31}\text{P}$ (sec)	$^{34}\text{Cl}^m \rightarrow ^{34}\text{S}$ (min)	$^{38}\text{Ca} \rightarrow ^{38}\text{K}$ (sec)
2.1 ± 0.3 ^a	4.15 ± 0.03 ^b	1.5 ± 0.1 ⁱ	2.40 ± 0.07 ^m	32.40 ± 0.04 ^q	0.439 ± 0.012 ^t
2.1 ± 0.1 ^b	4.149 ± 0.005 ^g	1.35 ± 0.10 ^j	2.61 ± 0.05 ⁿ	31.99 ± 0.05 ^r	0.430 ± 0.012 ^u
2.31 ± 0.02 ^c	4.083 ± 0.012 ^h	1.4 ± 0.1 ^b	2.56 ± 0.10 ^o	32.06 ± 0.08 ^s	
2.1 ± 0.2 ^d	4.084 ± 0.022 ^u	1.18 ± 0.04 ^k	2.605 ± 0.012 ^p	31.93 ± 0.09 ^u	
2.210 ± 0.021 ^e		1.210 ± 0.010 ^c	2.543 ± 0.008 ^h		
2.240 ± 0.010 ^u		1.22 ± 0.03 ^d	2.562 ± 0.007 ^u		
		1.181 ± 0.013 ^l			
		1.1783 ± 0.0048 ^u			
2.2345 ± 0.0090 ^v	4.117 ± 0.038 ^w	1.1786 ± 0.0045 ^v	2.562 ± 0.012 ^x	32.00 ± 0.04 ^y	0.435 ± 0.009 ^x

^aReference 77.^bReference 78.^cReference 39.^dReference 40.^eReference 41.^fReference 53.^gReference 54.^hReference 34.ⁱReference 79.^jReference 80.^kReference 81.^lReference 82.^mReference 83.ⁿReference 84.^oReference 85.^pReference 33.^qReference 63.^rReference 62.^sReference 56.^tReference 69.^uThis work.^vWeighted average of last two results.^wUnweighted average.^xWeighted average of all results.^yWeighted average of last three results.

thick, 4.3-mm-diam Ta discs which were then mounted in Be rabbits. The ^{25}Al activity was made by the $^{24}\text{Mg}(d, n)^{25}\text{Al}$ reaction with a 7.1-MeV beam of deuterons. A small amount of contaminant activity was made by the deuterons passing through a 25- μm Al foil which separated the rabbit system from the high vacuum in the beam pipe. Instead of air, argon pusher gas was used in the experiment to reduce contaminant positron activities produced in N_2 and O_2 . Spectra were

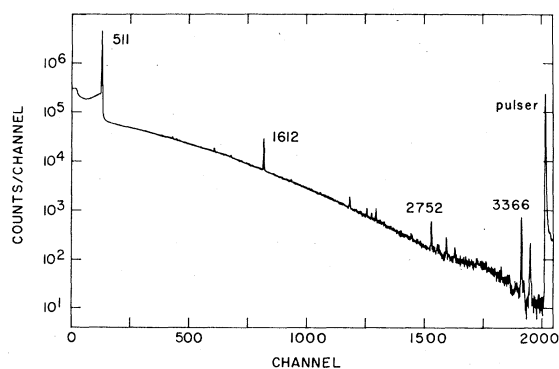


FIG. 3. The sum of the data from the ^{21}Na experiment measuring the intensity of the 2796-keV γ ray. This spectrum was taken in groups 1 and 2 (0-30 sec) of the data collection period. Note the contaminant lines at 2752 and 3366 keV due to ^{64}Ga and ^{66}Ga made by the (p, n) reaction in a Zn contaminant in the targets. The energy calibration is 1.601 keV/channel with a zero suppression of 188 channels. 3.2 cm of Pb absorber were used.

collected in 8 consecutive groups each lasting 5.0 sec.

Of the five runs carried out with three detector geometries, runs 1 to 3 were made using a large block of Lucite to trap the positrons and a 0.64-cm Pb absorber; run 4 was made with an alumi-

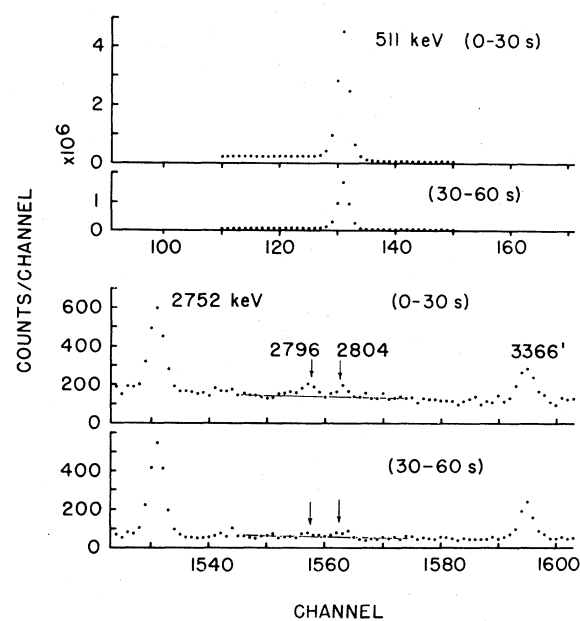


FIG. 4. Detailed plots of the 511- and 2796-keV peaks in the ^{21}Na experiment. The 0-30 sec data are the same as in Fig. 3.

num hutch and 0.64-cm Pb, and run 5 was made with the aluminum hutch, 0.64-cm Pb and 1.90 cm of Lucite between the Pb and the detector. Efficiency calibrations were made for each geometry with ^{22}Na and ^{56}Co . Including only the independent uncertainties in each geometry, the results for the absolute intensity (in percent) of the 1612-keV γ ray were 0.763 ± 0.020 (runs 1-3), 0.777 ± 0.023 (run 4), and 0.782 ± 0.024 (run 5). These values are in good agreement. Including additional efficiency-calibration uncertainties, common to the three geometries, the final value for the intensity of the 1612-keV γ ray is $(0.776 \pm 0.028)\%$. Four previous measurements of this intensity are all in agreement with this value and with each other: $(0.9 \pm 0.2)\%$, Makela *et al.*³⁶; $(0.7 \pm 0.2)\%$ Bardin *et al.*³⁷; $(0.84 \pm 0.07)\%$, Jundt *et al.*³⁸; and $(0.794 \pm 0.035)\%$, Azuelos *et al.*³⁴ The weighted mean of all five is $(0.788 \pm 0.021)\%$.

D. ^{26}Si decay

This decay has been studied several times previously (Refs. 39-41), but branches to the excited 1^+ states of ^{26}Al at 2739 and 3723 keV have not been reported.

The ^{26}Si activity was made in targets of natural magnesium by the $^{24}\text{Mg}(^3\text{He}, n)^{26}\text{Si}$ reaction using a 12.0-MeV ^3He beam and a 3.2-cm Pb absorber. Data were collected in two consecutive 2.3-sec

spectra. Table IV lists the relative intensities of the observed γ rays in ^{26}Si decay and comparisons with previous work. Our results agree well with earlier values except for the 1622-keV γ -ray relative intensity reported by Ref. 41. Determination of the 1622-keV peak area was somewhat complicated by interference from the 1612-keV γ ray emitted in the decay of ^{25}Al produced in the target and by the curved background in the 1622-keV region of the spectrum due to Compton scattering of the 1778-keV γ ray from ^{28}Al decay. Figures 5 and 6 show the γ -ray spectra.

To provide an absolute normalization for the branch intensities, the half-life of ^{26}Si was measured following the procedures described earlier. Five runs were made, with results in good agreement: the weighted average is 2.240 ± 0.010 sec. Table III lists previously reported values for the ^{26}Si half-life; for further calculations, we adopt 2.2345 ± 0.0090 sec, the weighted average of this result and the result reported by Ref. 41. Using the Coulomb corrections to the Fermi matrix element and the radiative corrections^{3,4} to the phase-space factor f_β , and correcting the value to take into account recent Q values²⁸, the partial half-life for the superallowed Fermi decay to the 228-keV 0^+ state in ^{26}Al was calculated to be 2.978 ± 0.014 sec.

Table I lists the absolute β branches and values

TABLE IV. Relative intensities of daughter γ rays in $^{26}\text{Si}(\beta^+\gamma)^{26}\text{Al}$.

E_γ (keV)	Transition		Relative intensity			
	Initial state	Final state	This work ^a	b	c	d
792	1850	1058	<2.7			
829	1058	228	1000.0 ± 5.2	1000	1000	1000
889	2739	1850	<2.0			
980	2739	1759	<1.6			
1014	2072	1058	e			
1342	1759	417	<0.98		<7	<20
1434	1850	417	<0.96			
1622	1850	228	124.5 ± 2.3	134 ± 5	149 ± 16	127 ± 7
1655	2072	417	1.45 ± 0.32			
1682	2739	1058	<0.58			
1843	2072	228	11.79 ± 0.27	16 ± 3	13 ± 3	12 ± 2
1873	3723	1850	<0.41			
1964	3723	1759	<0.38			
2322	2739	417	<0.28			
2511	2739	228	2.82 ± 0.10		<5	4.5 ± 1.5
2666	3723	1058	<0.15			
3306	3723	417	<0.064			
3495	3723	228	<0.045		<5	

^aUpper limits are 2σ confidence intervals (98% confidence).

^bReference 41.

^cReference 40.

^dReference 39.

^eObscured by the 1014-keV γ ray due to ^{27}Mg β^- decay.

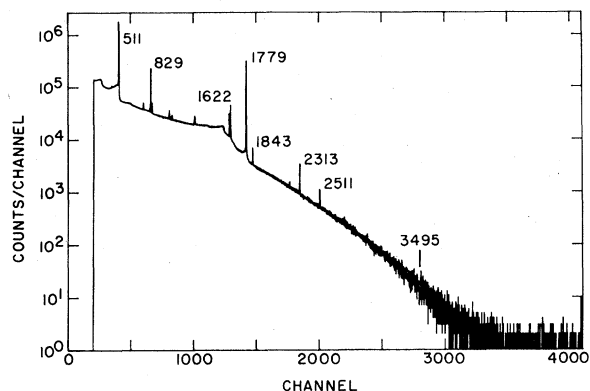


FIG. 5. The Ge(Li) spectrum accumulated in the first group (0-2.3 sec) in the ^{26}Si experiment. The energy calibration is 1.251 keV/channel. Peaks are labeled in keV. The 1779-keV peak is due to ^{28}Al decay and the 2313 to ^{14}O ; the other labeled peaks are due to ^{26}Si . 3.2 cm of Pb absorber were used.

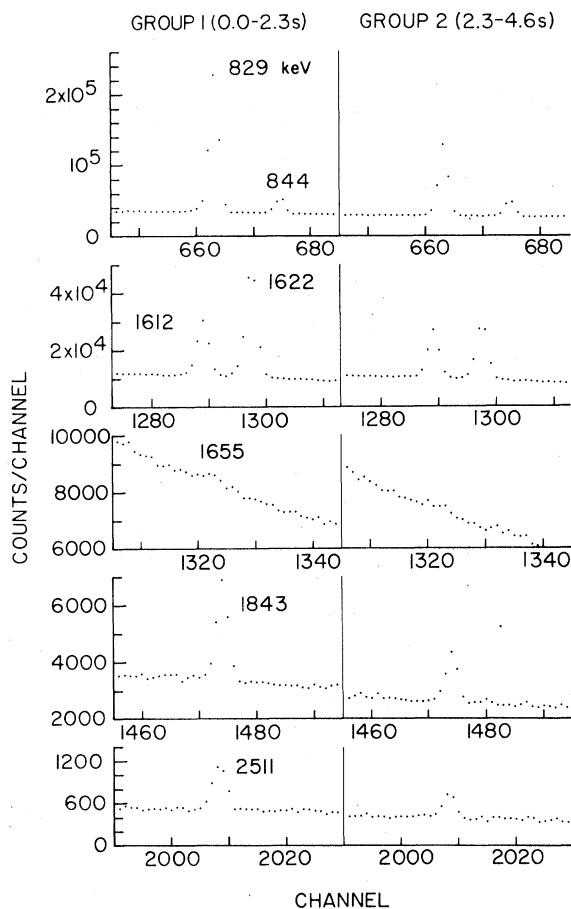


FIG. 6. Detailed Ge(Li) spectra of the peaks due to ^{26}Si decay. The group 1 data are the same as in Fig. 5. The 844-keV peak is due to ^{27}Mg and the 1612 to ^{25}Al .

of $\log ft$ derived from the measured half-life and from our relative γ -ray intensities. A $\log ft$ value is not included for the superallowed Fermi branch; in this analysis, we assumed a strength for this branch.

E. ^{29}P decay

The ^{29}P activity was made with a 5.5-MeV deuteron beam using the $^{28}\text{Si}(d,n)^{29}\text{P}$ reaction in targets of natural silicon mounted in aluminum rabbits. At the detector, the rabbits stopped in a Lucite hutch and 0.64 cm of Pb were used to reduce the 511-keV radiation by $\sim 60\%$. Data were collected in 16 consecutive groups of 3.20 sec (two runs) or in 16 groups of 6.40 sec (two runs). The time decay of the 511-keV peak was fitted with components having half-lives of 4.083 sec (^{29}P), 6.346 sec (^{26}Al), and 149.9 sec (^{30}P); no other significant component was found. A run to search for long-lived components, by recording spectra in 16 groups of 32 sec each, showed only ^{30}P activity. Interference with the 1273-keV γ ray by the single-escape peak of the 1778-keV γ ray emitted in the decay of ^{28}Al was treated by fitting the area of the 1273-keV peak with 4.083 sec and the 134.8 sec components. Using the procedures described earlier and including only the statistical error in the 1273- and 511-keV peak areas, the four runs gave the following values for the absolute intensity of the 1273-keV γ ray: $(1.295 \pm 0.023)\%$, $(1.332 \pm 0.022)\%$, $(1.334 \pm 0.052)\%$, and $(1.331 \pm 0.023)\%$. Combining the weighted average with the efficiency-calibration uncertainty of $\pm 1.4\%$ gives an absolute intensity of $(1.320 \pm 0.022)\%$.

The intensity of the 1273-keV γ ray has been measured several times: Roderick *et al.*⁴² obtained $(0.80 \pm 0.20)\%$, Lönsjö⁴³ $(1.2 \pm 0.2)\%$, and Azuelos *et al.*³⁴ $(1.62 \pm 0.28)\%$. Since the result of our work is much more precise than any of the previous results, we adopt our value alone instead of a weighted average.

The 511-keV peak was also analyzed to extract the ^{29}P half-life using the technique described earlier. The results of the four runs did not show good agreement: the two runs with 3.2-sec groups gave 4.057 ± 0.026 sec and 4.124 ± 0.027 sec, while the two runs with 6.4-sec groups gave 4.132 ± 0.054 sec and 4.058 ± 0.028 sec. The weighted average is 4.084 ± 0.022 sec where the uncertainty has been increased to reflect the poor agreement of the four runs. The value is compared with other results in Table III. In the absence of a basis for choice among the conflicting results, we use the unweighted average, 4.117 ± 0.038 sec, in calculations of $\log ft$ values in Tables I and II.

An additional run with 1.9 cm of Pb absorber was made in order to search for high-energy γ

rays. With the same target and beam, data were collected in two groups of 4.0 sec. Relative to the 1273-keV γ ray, the intensities of the 1152-, 2028-, and 2426-keV γ rays were 0.0492 ± 0.0033 , $< 3.3 \times 10^{-3}$, and 0.2945 ± 0.0073 , respectively. Table I lists the absolute β branches and compares with earlier results.²⁸ The second-forbidden branch to the $\frac{5}{2}^+$ state at 2028 keV is included to emphasize that our result disagrees with that of Ref. 34 which reports a strong branch ($0.2 \pm 0.1\%$) to the 2028-keV level.

F. ^{30}P decay

The reaction $^{27}\text{Al}(\alpha, n)^{30}\text{P}$, with a 10.0-MeV α beam and a 0.25-mm-thick target of 99.999% pure aluminum, produced the ^{30}P activity. The target was carried by hand from the bombarding station to the Ge(Li) detector.

A search was made for weak γ rays following allowed electron-capture transitions to ^{30}Si states at 3499, 3770, and 3788 keV. The 3788-keV 0^+ state decays to the 2235-keV level emitting a 1552-keV γ ray. 1.7 cm of aluminum plus 2.5 cm of Pb absorber was placed between target and detector. The bombarded side of the target faced away from the detector, allowing $\sim 50\%$ of the positrons to escape, and thus reducing the count rate. Spectra were taken in two groups of 200 sec. Initial runs showed that the high-energy background was due largely to pileup, so pileup rejection was used in part of the experiment. A calibration spectrum, taken in coincidence with the veto signal of the pileup-rejection system showed that the system did not reject photopeak counts and distort the spectrum. γ rays at 1552-, 3499-, and 3770-keV were observed with intensities of 0.0569 ± 0.0038 , 0.01175 ± 0.00075 , and $(1.32 \pm 0.23) \times 10^{-3}$ relative to the 2235-keV γ ray (see Figs. 7 and 8). The assignment of the 3770-keV γ ray to ^{30}P decay was somewhat uncertain because the peaks were too weak for a definitive half-life determination ($t_{1/2} = 165 \pm 81$ sec results from the data in Fig. 8).

We also measured the absolute intensity of the 2235-keV γ ray. In this measurement, the ^{30}P activity was completely surrounded by aluminum in order to trap all of the positrons. Two detector geometries were used: one run was made with 1.7 cm of aluminum and 0.64 cm of lead absorber and two runs were made with an additional 1.9 cm of Lucite between the lead and the detector. A ^{22}Na source was prepared in an unused target and mounted in the same geometry in order to measure the 511-keV efficiency. A calculated 4.9% of the ^{30}P positrons and 0.8% of the ^{22}Na positrons annihilate in flight. Data were collected in 4 groups of 150 sec each, although

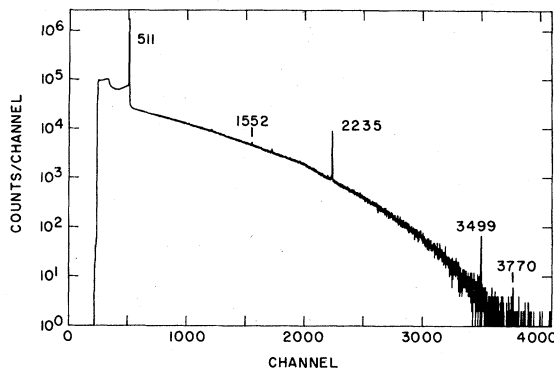


FIG. 7. The Ge(Li) spectrum taken in group 1 (0-200 sec) in the ^{30}P experiment with pileup rejection. The energy calibration is 1.001 keV/channel. Peaks are labeled in keV. 1.7 cm of Al and 2.5 cm of Pb absorber were used.

multiscaling was hardly necessary since at least 99.9% of the 511-keV radiation was due to ^{30}P . The absolute intensities from the two geometries were in good agreement: $(5.61 \pm 0.50) \times 10^{-2}\%$ and $(6.05 \pm 0.35) \times 10^{-2}\%$ (only the independent uncertainties are quoted). Including a common error in efficiency calibration gives a final result of $(5.91 \pm 0.30) \times 10^{-2}\%$, in agreement with Alburger and Goosman⁴⁴ who obtained $(6.1 \pm 0.6) \times 10^{-2}\%$,

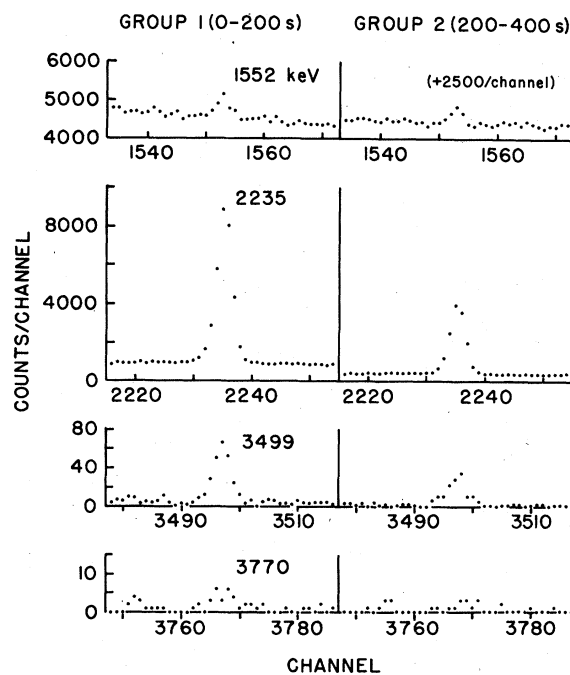


FIG. 8. Detailed spectra of the peaks due to ^{30}P decay. The group 1 data are the same as in Fig. 7. 2500 counts/channel have been added to the spectrum for the 1552-keV ray in the second group in order to simplify the plot.

but in disagreement with Gourlay *et al.*⁴⁵ who reported $(8.7 \pm 0.9) \times 10^{-2}\%$. It was noted by Alburger and Goosman that detection efficiency was difficult to determine in the geometry used by Gourlay *et al.* To calculate absolute branches, we adopt the weighted average of Alburger and Goosman and this work, $(5.95 \pm 0.27) \times 10^{-2}\%$.

The β -branch intensities listed in Table I use the γ -ray branching ratios given in Ref. 28.

G. ^{30}S decay

The experimental procedure was essentially the same as for ^{26}Si . A natural silicon target, mounted in an aluminum rabbit, was bombarded by a 10.0-MeV ^3He beam which produced ^{30}S activity by the reaction $^{28}\text{Si}(^3\text{He}, n)^{30}\text{S}$.

In the first part of the experiment, the daughter γ -ray intensities were measured relative to the intensity of the 677-keV γ ray emitted in the superallowed Fermi branch from the 0^+ ground state of ^{30}S . Spectra were collected in two groups of 1.3 and 1.5 sec. Special care was required in this case in determining the relative photopeak efficiencies at 677 and 709 keV because of the use of 1.9 cm Pb absorber. Our procedure was to measure the relative efficiency at 570 keV, 847 keV, and above, using ^{207}Be and ^{56}Co sources. Then interpolation between 570 and 847 keV was done assuming that the relative efficiency at energy E_γ of the shielded cylindrical detector was given by the following expression:

$$\text{eff}(E_\gamma) = \frac{A}{E_\gamma^\alpha} \int_{\text{detector}} T_0^{1/\cos\theta} [1 - \exp[-\mu l(\theta)]] \sin d\theta.$$

Here T_0 is the total probability for a photon with energy E_γ to reach the detector traveling along the detector's axis, $l(\theta)$ is the thickness of germanium along a path at an angle θ to the detector's axis, and μ is the attenuation coefficient for photons with energy E_γ in germanium. Parameters A and α were adjusted to match the measured relative efficiencies at 570 and 847 keV. Extrapolation to 1000 keV gave good agreement with the measured relative efficiency, so we had confidence in this expression's ability to predict the 677- and 709-keV relative photopeak efficiencies. Table V lists the relative γ -ray intensities measured in this work and compares to previous results.

The absolute normalization was carried out by measuring precisely the half-life of ^{30}S . Spectra were collected in 16 consecutive 400 ms groups. The half-life was extracted from the data by correcting the areas of the 677-keV peak for dead-time and pileup losses and then fitting to an exponential. Five runs were made with only slight

differences (up to 30%) in count rate and a sixth run was made at about twice the count rate of the first five. The results of the six runs were 1.1943 ± 0.0099 sec, 1.1868 ± 0.0098 sec, 1.1619 ± 0.0092 sec, 1.1774 ± 0.0093 sec, 1.1757 ± 0.0086 sec (all at a count rate of 4000–5000 per sec in the first group), and 1.1772 ± 0.0102 sec (at ~ 10000 per sec). The weighted average of the results is 1.1783 ± 0.0048 sec, where the uncertainty has been increased in view of the somewhat excessive scatter among the six results. Table III lists the results of this and previous measurements. Our adopted "best value" is 1.1786 ± 0.0045 sec. The partial half-life of the superallowed Fermi branch was taken to be 1.5485 ± 0.0067 sec.

The absolute β -branch intensities and $\log ft$ values, deduced from our relative intensities, and the best-value half-life are listed in Table I. We note that these results indicate a violation of mirror symmetry in the Gamow-Teller transitions between the ground states of ^{30}Si , ^{30}P , and ^{30}S . After extracting spin factors, the ^{30}S decay to the ground state of ^{30}P is $8.4 \pm 3.5\%$ faster than the ^{30}P decay to the ground state of ^{30}Si . This is perhaps not surprising considering the difference in the binding energies of ^{30}S and ^{30}Si (11.9 MeV) and the prediction by Hardy and Towner³ and by Raman *et al.*⁴ of a Coulomb correction of 0.6 to 1.1% in the Fermi decay of ^{30}S . The difference in the GT rates would be explained if the ground state of ^{30}S consisted of |analog of $^{30}\text{Si}(\text{g.s.})\rangle + 0.028$ |analog of ^{30}Si (first excited 0^+ state)\rangle.

H. ^{31}S decay

The ^{31}S activity was made by the $^{31}\text{P}(p, n)^{31}\text{S}$ reaction with 11.0-MeV protons in targets of MnP powder wrapped in 25- μm Ta foil and mounted in Be rabbits.

The measurement of the relative intensities of the daughter γ rays used a 1.9-cm Pb absorber and pileup rejection. That the pileup-rejection system did not affect the relative efficiency in a count-rate dependent way was established by checking that the spectrum of rejected pulses did not show peaks and also by measuring the detector's relative efficiency at two different counting rates. Since a ^{66}Ga source, made by $^{66}\text{Zn}(p, n)^{66}\text{Ga}$ in a ZnP target identical to the ones used in the experiment, was used to calibrate the detector, this was easily accomplished by making two calibration runs ~ 11 h apart. The relative intensities of γ rays obtained here are listed in Table VI and compared to previous results.⁴⁶

We also remeasured the absolute intensity of the 1266-keV γ rays in order to normalize the excited-state intensities. This was done in the same manner as in the ^{21}Na and ^{29}P experiments, using

TABLE V. Relative intensities of daughter γ rays in $^{30}\text{S}(\beta^+\gamma)^{30}\text{P}$.

E_γ ^a (keV)	Transition ^a		Relative intensity		
	Initial state	Final state	This work ^b	c	d
677	677		1000 ± 12	1000	1000
709	709		3.74 ± 0.88	6 ± 3	7.2 ± 2.1
745	1454	709	<1.6		
990	3927	2938	<0.94		
1454	1454		<0.56		
1484	2938	1454	<0.47		
1565	3019	1454	<0.44		
1850	3304	1454	<0.47		
2261	2938	677	<0.30		
2277	3731	1454	<0.30		
2310	3019	709	^e		
2341	3019	677	29.00 ± 0.55	33 ± 2	27.5 ± 2.0
2370	4343	1973	<0.28	<0.65	
2473	3927	1454	<0.49		
2595	3304	709	<0.44		
2627	3304	677	<0.30		
2781	4235	1454	<0.44		
3019	3019		0.125 ± 0.061		
3022	3731	709	<0.26		
3047	4501	1454	<0.18		
3054	3731	677	<0.27		
3218	3827	709	<0.13		
3250	3927	677	<0.11		
3304	3304		<0.15		
3526	4235	709	<0.079		
3558	4235	677	<0.13		
3731	3731		<0.065	<0.55	
3759	4468	709	<0.073 ^f		
3792	4501	709	<0.061		
3824	4501	677	<0.059		
3927	3927		<0.057		
4235	4235		<0.045		
4343	4343		<0.038		
4468	4468		<0.043 ^f	<2.7	
4501	4501		<0.042	<2.7	

^a Level energies from Ref. 28.^b 2σ upper limits (98% confidence).^c Reference 40.^d Reference 39.^e Obscured by ^{14}O γ ray at 2313.^f Following Fermi transition to nonanalog 0^+ state.

8 multiscaled groups with a 2.00-sec dwell time for the first three runs and 16 groups of 2.40 sec for a further two runs. (The last two runs were also analyzed to determine the half-life of ^{31}S .) All runs were made with the same detector geometry: a Lucite hutch to trap the positrons and a 0.64-cm Pb absorber. The count rate was varied by a factor 1.6. Assuming a ^{31}S half-life of 2.564 sec and including only the statistical error in peak areas, the absolute intensities of the 1266-keV γ ray from the five runs were (1.124 ± 0.022)%, (1.073 ± 0.021)%, (1.077 ± 0.020)%, (1.067 ± 0.029)%, and (1.087 ± 0.031)%. The data were

also analyzed assuming a 2.543-sec half-life for ^{31}S and the resulting estimate of the 1266-keV intensity was 0.32% higher. This uncertainty and a further 1.4% due to the efficiency calibration combined with the weighted average of the five runs gives our result: (1.087 ± 0.021)%. Measurements of the 1266-keV intensity have been reported previously by Talbert and Stewart,⁴⁷ (1.1 ± 0.1)%; Alburger,³³ (1.25 ± 0.06)%; and Azuelos *et al.*,³⁴ (0.98 ± 0.20)%. The weighted average of these results is (1.103 ± 0.033)%, where the discrepancy between Alburger's result and ours has been taken into account by increasing the un-

TABLE VI. Relative intensities of γ rays emitted in $^{31}\text{S}(\beta^+\gamma)^{31}\text{P}$.

E_γ ^a (keV)	Transition ^a		Relative intensity	
	Initial state	Final state	This work ^b	c
1266	1266		1000 ± 20	1000
1868	3134	1266	< 1.7	
2234	2234		< 0.64	< 7
2240	3506	1266	4.35 ± 0.69	
2360	4594	2234	< 0.74	
2995	4261	1266	d	
3134	3134		28.80 ± 0.81	28 ± 4
3327	4594	1266	< 0.56	
3506	3506		6.62 ± 0.44	10 ± 3
4261	4261		< 0.18	
4594	4594		< 0.051	

^aLevel energies from Ref. 28.

^b2 σ upper limits (98% confidence). The uncertainty in the 1266-keV relative efficiency is included only in the relative intensity of the 1266-keV γ ray.

^cReference 46.

^dObscured by the single-escape peak of the 3506-keV γ ray.

certainty in the average; we adopt this value in further calculations.

The areas of the 511-keV peaks in the two runs made with 16 groups of 2.400 sec each were also analyzed to determine the half-life of ^{31}S . The ^{31}S activity was quite pure, accounting for > 99.5% of the positron activity at the start of the counting cycle, and because the decay was followed for only fourteen half-lives, we were unable to determine the half-life of the long-lived background. To overcome this problem the 511-keV peak was fitted assuming ^{11}C , ^{13}N , ^{14}O , or ^{11}C and ^{14}O components in the long-lived activity. Poor fits were obtained assuming only ^{14}O and the other three choices gave the same half-life for ^{31}S . Also, other short-lived components, ^{35}Ar , ^{27}Si , ^{23}Mg , and ^{19}Ne , were included but it was found that this did not improve the fits significantly. A leaky integrator was not used in this case, but the count rate was monitored and, because the accelerator's beam was stable, the count rate varied less than $\pm 15\%$ from cycle to cycle. The first run, with $\sim 10\,500$ counts/sec at the start of the counting period, gave a half-life of 2.562 ± 0.008 sec, and the second, at ~ 8000 counts/sec, gave 2.562 ± 0.010 sec. The weighted average, 2.562 ± 0.007 sec, disagrees with the two previous precise values of 2.605 ± 0.012 sec,³³ and 2.543 ± 0.007 sec.³⁴ Reference 28 lists ten measurements of the half-life of ^{31}S reported during the past 30 years. We reviewed all of these measurements before calculating a best value. Five of the measurements were

rejected for the following reasons. Reference 48 had to make large ($\sim 100\%$) dead-time corrections to their data and they determined the high-count-rate response of their apparatus with a ^{62}Cu source which they believed had a 10.1 min half-life rather than 9.72 ± 0.02 min adopted in 1979. Consequently, their dead-time corrections had to be wrong. References 49–52 all reported several half-life measurements in addition to ^{31}S . In each case, these additional values deviated so badly from the best values available in 1979 that these results were rejected as unreliable. The five results not rejected are shown in Table III. The weighted average of the six results is 2.562 ± 0.012 sec, where the uncertainty has been increased to take account of the poor agreement of these measurements. This value was used to calculate the $\log ft$ values in Table I.

I. ^{33}Cl decay

In the relative-intensity part of the measurement, the ^{33}Cl activity was made by the $^{32}\text{S}(d,n)^{33}\text{Cl}$ reaction with 11.0-MeV deuterons on thick targets of natural sulfur. Because elemental sulfur evaporates under bombardment, gas-tight aluminum rabbits were used. A 4.5-cm Pb absorber reduced the detector's sensitivity to annihilation radiation. Data were recorded in two groups of 2.5 sec which made it possible to separate the 841-keV peak due to ^{33}Cl decay from the 843-keV peak due to ^{27}Mg produced in the aluminum-alloy rabbit. Figures 9 and 10 show Ge(Li) spectra collected in this experiment and Table VII lists the relative γ -ray intensities and compares with the previous results of Bardin *et al.*³⁷ We report four previously unobserved

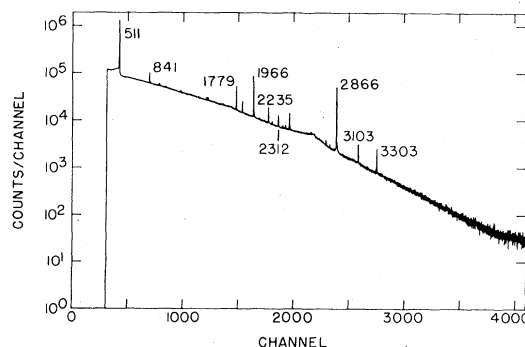


FIG. 9. The Ge(Li) spectra collected in group 1 (0.0 to 2.5 sec) in the ^{33}Cl experiment. A 4.5-cm Pb absorber removed most of the 511-keV radiation. The energy calibration is 1.200 keV/channel. Peak energies are given in keV. Prominent contaminant peaks are labeled at 1779 keV (^{28}Al), 2235 keV (^{30}P), 3103 keV (^{37}S), and 3303 keV ($^{34}\text{Cl}^m$). All of the peaks have been identified except for a small long-lived peak at 2025 keV.

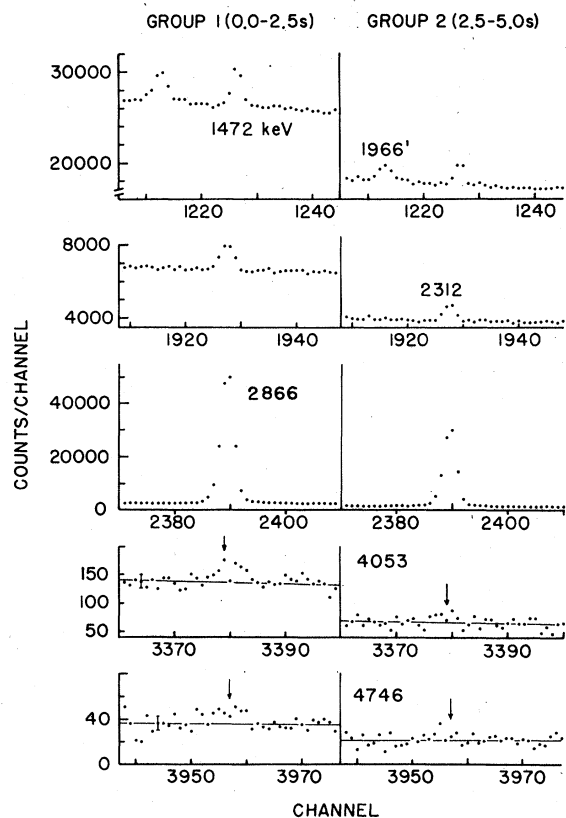


FIG. 10. Detailed spectra of γ -ray peaks due to ^{33}Cl decay. The group 1 data are the same as in Fig. 9. The arrows indicate the 4053- and 4746-keV peak centroids calculated from the energy calibration; the solid lines indicate linear backgrounds.

γ rays.

A 2312-keV γ ray also appears in the β^+ decay of ^{14}O (half-life = 70.6 sec) which could be made with an 11-MeV deuteron beam only by $^{14}\text{N}(d, 2n)^{14}\text{O}$, with threshold at $E_d = 9.3$ MeV. Experimental cross sections for this reaction have not been reported, but in view of the other channels available with positive Q values [$^{14}\text{N}(d, n)^{15}\text{O}$, $Q = 5.07$ MeV; $^{14}\text{N}(d, p)^{15}\text{N}$, $Q = 8.61$ MeV; $^{14}\text{N}(d, \alpha)^{12}\text{C}$, $Q = 13.57$ MeV, etc.], we assume that ^{14}O contamination was negligible. Thus, the relative intensity for the 2312-keV γ ray given in Table VII was deduced from the data assuming no contribution from ^{14}O decay. A separate analysis of the data, taking advantage of the fact that data were collected in two groups, showed that if a contribution from ^{14}O were to be included as an additional free parameter, then the intensity of the 2312-keV γ ray relative to the 2866-keV γ ray would be changed from 0.0231 ± 0.0014 to 0.0212 ± 0.0033 .

The evidence for the γ rays at 4053 and 4746 keV is weak because distinct photopeaks are not

TABLE VII. Relative intensities of daughter γ rays in $^{33}\text{Cl}(\beta^+\gamma)^{33}\text{S}$.

E_γ ^a (keV)	Transition		Relative intensity	
	Initial state	Final state	This work ^b	^c
841	841		1186 ± 36	960 ± 120
1125	1966	841	13.8 ± 3.4	
1472	2312	841	57.9 ± 3.3	<44
1519	3832	2312	<5.2	
1966	1966		1042 ± 16	1000 ± 70
2026	2866	841	15.4 ± 1.9	
2312	2312		23.1 ± 1.4 ^d	
2409	4375	1966	<3.6	
2866	2866		1000 ± 18	1000 ± 70
3094	3935	841	<3.0	
3212	4053	841	<1.3	
3534	4375	841	<0.96	
3584	4424	841	<0.90	
3832	3832		<1.2	
3905	4746	841	<0.68	
3935	3935		<0.95	
4053	4053		1.08 ± 0.31	
4144	4144		<0.58	
4375	4375		<0.99	
4424	4424		<0.67	
4746	4746		0.85 ± 0.23	

^a Level energies from Ref. 28.

^b 2σ upper limits (98% confidence).

^c Reference 37.

^d Assuming no contamination from ^{14}O decay.

seen. Nevertheless, the net area calculated using a linear background is more than 3.4 standard deviations from zero in both cases and therefore the probability of this happening by chance in these particular regions of the spectrum is $<0.1\%$ for each peak. Further, the areas in the two groups do not disagree with each other (i. e., we are not seeing a bump in only one group).

The absolute intensities of the 1966- and 2866-keV γ rays were measured, as described previously, by comparing γ -ray intensities with positron annihilation radiation. Targets of PbS evaporated on 0.38-mm-thick discs of Ta were mounted in Be rabbits. The activity was made by the (d, n) reaction with 6.0- and 5.3-MeV beams of deuterons and data were collected in 8 consecutive groups each lasting 1.8 sec. Three runs were made using an aluminum hutch to trap the positrons plus 0.64 cm of Pb absorber, and a fourth run was made with 1.9 cm of Lucite placed between the Pb and the detector. In each run, the time decay of the 511-keV peak was fitted with components of 2.511-sec half-life (^{33}Cl), 64.6 sec (^{17}F), and 149.9 sec (^{30}P). One of the first three runs was rejected because the least squares fit yielded a large value of χ^2 ($\chi^2 = 36$ for 5 degrees of freedom). No systematic trend could be ob-

served in the residuals of the rejected fit, so the presence of an unknown contaminant was not indicated. A rough estimate showed that $<6\%$ of the short-lived positron activity would be due to ^{34}Cl made in the 0.75% abundant ^{33}S in natural sulfur, so an adjustment of $(3 \pm 3)\%$ was made to the area of the 511-keV peak. The 1966-keV γ -ray intensity was $(0.462 \pm 0.032)\%$ without Lucite and $(0.426 \pm 0.035)\%$ with Lucite. The corresponding results for the 2866-keV γ ray were $(0.422 \pm 0.028)\%$ and $(0.402 \pm 0.031)\%$. The averages, including systematic uncertainties common to both geometries, are $(0.448 \pm 0.027)\%$ for 1966 keV and $(0.414 \pm 0.024)\%$ for 2866 keV. These numbers have a common uncertainty of 0.021% (i. e., $\sim 5\%$ of the measured intensities). From the relative intensities of the 1966- and 2866-keV γ rays in Table VII, the factor for converting relative γ -ray intensities to absolute intensities is found to be $(4.20 \pm 0.24) \times 10^{-6}$.

Bardin *et al.*³⁷ reported an absolute intensity of $(0.560 \pm 0.059)\%$ for the 2866-keV γ ray. Since they made no mention of in-flight-annihilation, which we found to be $(7.0 \pm 0.1)\%$ of the total positron annihilation, we reduce their number by this amount. Thus their factor for converting relative γ -ray intensities to absolute intensities is $(5.21 \pm 0.55) \times 10^{-6}$, in disagreement with this work. The weighted average of the two factors is $(4.36 \pm 0.56) \times 10^{-6}$, where the error has been increased to account for the poor agreement. We use this combined value to calculate the β branches and $\log ft$ values shown in Table I.

For the half-life of ^{33}Cl , we used 2.511 ± 0.004 sec, the weighted average of the values reported by Scanlon and Crabtree,⁵³ Tanihata *et al.*,⁵⁴ and Azuelos *et al.*³⁴ We did not include values reported by Muller *et al.*⁵⁵ and by Jänecke⁵⁰ because other half-lives presented in these papers show serious disagreement with more accurate values available in 1979.

J. ^{34}Cl and $^{34}\text{Cl}^m$ decay

The purpose of this experiment was to search for a weak Gamow-Teller branch in the β^+ decay of ^{34}Cl (g.s.) and also to remeasure the intensities of the electron-capture branches in $^{34}\text{Cl}^m$ decay reported previously by Van Driel *et al.*⁵⁶ The $^{34}\text{Cl}^m$ activity was made by the reaction $^{31}\text{P}(\alpha, n)^{34}\text{Cl}$ using 10- and 11-MeV α beams and targets of MnP powder pressed into 0.64-cm diameter holes in Be, Zr, and Al targets. The activity was carried from the bombarding station to the detector by hand.

In the search for weak high-energy γ rays, pile-up rejection was used to reduce the background. Data were collected in two consecutive groups

lasting 1500 sec each and a plot of the ratio (area group 1)/(area group 2) against γ -ray energy for the four strong photopeaks in $^{34}\text{Cl}^m$ decay (at 1176, 2127, 3303, and 4114 keV) showed no evidence for a significant departure from a constant (the weighted average of the four ratios had $\chi^2 = 2.68$ for 3 degrees of freedom). Since the only difference between the two groups was a change in count rate by a factor 1.72, we conclude that there is no count-rate-dependent distortion of the spectrum.

Most of the spectra were taken with a 2.5 cm Pb absorber to reduce the intensity of the 511-keV radiation. In order to measure the relative intensity of the 146-keV γ ray emitted in the $M3\gamma$ decay to the ^{34}Cl (g.s.), four runs were made with no Pb absorber and no positron stopper and at a source-to-detector distance of 12.0 cm [at this distance the Ge(Li) crystal covered 1.1% of a sphere]. A small summing correction was made in this case to take into account positrons which entered the detector. The relative photopeak efficiency calibrations were made using sources of ^{182}Ta (made by thermal neutron capture in 6.4- μm -thick Ta foil), ^{56}Co , and $^{14}\text{N}(p, \gamma)^{15}\text{O}$.

Table VIII lists the relative intensities of γ rays deduced from our experiment and from that of Van Driel *et al.*⁵⁶ We have adjusted their results to take into account the error in the Camp and Meredith¹² results for the relative intensities of high-energy γ rays in ^{56}Co and ^{66}Ga (see McCallum and Coote¹³) and also the differences in ^{182}Ta relative intensities reported by Meyer¹⁴ (used herein) and White *et al.*³⁷ (used by Van Driel *et al.*). The agreement is good. The upper limit on the relative intensity of the 4074-keV γ ray is the result of three separate experiments; the other values are the result of one experiment. In the runs to measure the 4074-keV intensity, we measured its peak area relative to the area of the 4114-keV γ ray so variations of detector relative efficiencies and distortion due to the pileup-rejection system were unimportant.

In order to determine the absolute branching in the competing γ and β decays of $^{34}\text{Cl}^m$, the internal-conversion coefficient for the $M3$ transition to the ground state must be known. The only precise measured value of this coefficient is 0.100 ± 0.009 , reported by Ward and Kuroda,⁵⁸ which disagrees with the calculated value of 0.172 ± 0.005 given by Band *et al.*⁵⁹ However, this γ transition is highly hindered, having a strength of only 1.6×10^{-6} W.u., so the difference could be attributed to the "penetration effect" (see Church and Weneser⁶⁰ and Green and Rose⁶¹). We adopt the Ward and Kuroda value in spite of the disagreement.

The $^{34}\text{Cl}^m$ half-life was measured by collecting

TABLE VIII. Relative intensities of γ rays in $^{34}\text{Cl}^m$ decay.

E_γ ^a (keV)	Transition		Relative intensities	
	Initial state	Final state	This work ^b	c
146	$^{34}\text{Cl}^m$	$^{34}\text{Cl}(0)$	944 ± 14	956 ± 19
1176	3303	2127	329.0 ± 2.8	322 ± 10
1385	4688	3303	< 0.21	
1573	4876	3303	0.37 ± 0.12	0.26 ± 0.05
1586	4889	3303	< 0.18	< 0.15
1987	4114	2127	4.31 ± 0.15	4.09 ± 0.15
2127	2127		1000 ± 11	1000
2560	4688	2127	0.783 ± 0.067	0.72 ± 0.14
2748	4876	2127	0.521 ± 0.066	0.49 ± 0.05
2762	4889	2127	< 0.11	
3303	3303		287.3 ± 3.1	273 ± 9
4074	4074		< 0.0081	< 0.023
4114	4114		6.37 ± 0.14	6.1 ± 0.4
4876	4876		< 0.0076	< 0.010
4889	4889		< 0.015	< 0.010

^a Level energies from Ref. 28. Except for the 146-keV γ ray, the transitions are between ^{34}S states.

^b 2σ upper limits (98% confidence). The uncertainty in the 2127-keV relative efficiency is included only in the relative intensity of the 2127-keV γ ray.

^c Reference 56; they used Ref. 12 for ^{56}Co relative intensities and Ref. 57 for ^{182}Ta intensities. The relative intensities of the 146-keV γ ray and the γ rays above 2800 keV have been recalculated using Ref. 14 for ^{182}Ta and applying the correction factor of Ref. 13 for ^{56}Co .

γ -ray spectra in 16 sequential groups with a dwell time of 1500 sec. A constant-rate pulser was fed into the Ge(Li) preamp to monitor dead-time and pileup losses from the 2127- and 3303-keV peaks which were used in the analysis. Both peaks were fitted well by the exponential. The result of the analysis is that the half-life of $^{34}\text{Cl}^m$ is 31.93 ± 0.09 min. Table III lists values reported previously. The weighted average of the three latest results is 32.00 ± 0.04 min which we use to calculate $\log ft$ values. The absolute β -branch intensities and $\log ft$ values determined using only our relative intensities are listed in Table I and are compared to shell-model calculations in Table II.

K. ^{35}Ar decay

A preliminary report of this work has been made previously⁶⁴; the branch intensities reported here supersede the earlier values.

The radioactivity was made by the $^{35}\text{Cl}(p, n)^{35}\text{Ar}$ reaction using 11-MeV protons and targets of LiCl and PbCl₂ wrapped in 25- μm Ta foil and mounted in Be rabbits. A 2.5-cm Pb absorber was inserted. Spectra were recorded in two consecutive groups of 1.8 sec. This investigation revealed the existence of two previously unreported branches in the decay of ^{35}Ar to states at 3918 and 3968 keV and determined an upper limit on the branch to the 4624-keV level. Figures 11

and 12 show the Ge(Li) spectra; Table IX lists the relative intensities of the γ rays from this and previous work.

We also remeasured the absolute intensity of the 1219-keV γ ray by monitoring the 511-keV radiation. Positrons were trapped in a Lucite hutch and only 0.64 cm of Pb absorber was used. Data

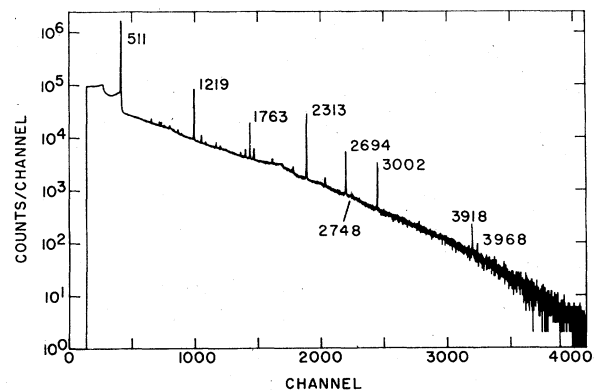


FIG. 11. The sum of all data collected in group 1 (0.0-1.8 sec) in the ^{35}Ar experiment. The energy calibration is 1.225 keV/channel. A 2.5-cm Pb absorber was used. All of the labeled peaks are due to ^{35}Ar γ rays except for the 2313-keV peak from ^{14}O . All of the peaks have been identified except for weak peaks at 1158 and 1483 keV.

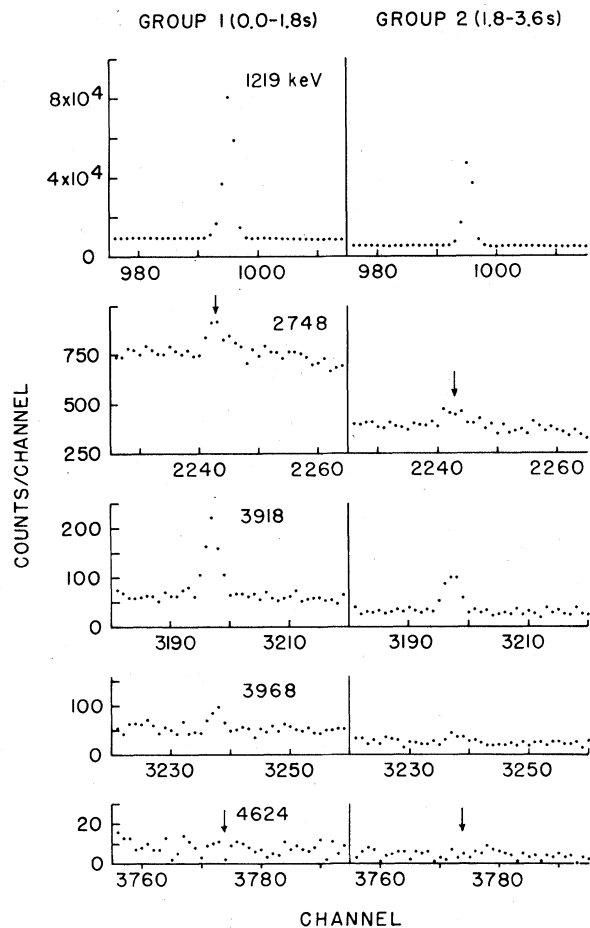


FIG. 12. Detailed spectra of some of the peaks due to ^{35}Ar γ rays. Arrows indicate the photopeak positions calculated from the energy calibration. The group 1 data are the same as in Fig. 11.

were recorded in four consecutive groups each lasting 1.000 sec. To extract the part of the 511-keV peak due to ^{35}Ar decay, the ratio (area 511)/(area 1219) in group n was fitted with the two-parameter expression $A_0 + \beta^n A_1$, where $\beta = 2^{1.000 \text{ sec}/1.773 \text{ sec}}$, which assumes only long-lived contaminants. Then A_0 is the ratio of the ^{35}Ar 511-keV peak area to the 1219-keV peak area. Two runs were made in slightly different geometries, with an extra 1.4 cm of Lucite inserted between the source and the Pb absorber in the second run. In both cases, the two-parameter fits to the four-point decay curves gave acceptable values of χ^2 (2.0 in run 1 and 2.5 in run 2, both for 2 degrees of freedom), which indicates that other short-lived activities made only negligible contributions to the total 511-keV radiation. Efficiency calibrations were made using ^{22}Na and ^{56}Co sources and the small corrections discussed earlier were made (absorption of the 511-keV radiation in the

PbCl_2 target was included in the calculation). The two runs gave values for the absolute intensity of $(1.191 \pm 0.042)\%$ and $(1.256 \pm 0.038)\%$ with a common systematic uncertainty of $(\pm 0.014)\%$; the weighted average is $(1.228 \pm 0.030)\%$. Four measurements of this intensity have been reported previously: $(1.223 \pm 0.046)\%$ (Wick *et al.*⁶⁵), $(1.22 \pm 0.20)\%$ (Geiger and Hooton⁶⁶), $(1.55 \pm 0.15)\%$ (Azuelos *et al.*³⁴), and $(1.34 \pm 0.08)\%$ (Hagberg *et al.*⁶⁷). The weighted average of these results and our value is $(1.244 \pm 0.033)\%$, where the uncertainty has been increased to take account of the scatter among the results ($\chi^2 = 6.11$ for 4 degrees of freedom). This weighted average is used to calculate absolute branch intensities.

For the half-life of ^{35}Ar , we use 1.773 ± 0.003 sec, the weighted average of the results of Wick *et al.*,⁶⁵ 1.770 ± 0.006 sec, and Azuelos *et al.*,³⁴ 1.774 ± 0.003 sec. The result of Jänecke,⁵⁰ 1.79 ± 0.01 sec, was not included because several other half-lives reported in the same paper showed serious discrepancies with the best values available in 1979. Also the result of Geiger and Hooton,⁶⁶ 1.787 ± 0.012 sec, was not used because of the poor consistency of the 8 measurements used to derive the reported result.

Table I lists the $\log ft$ values and absolute β branches deduced from our relative γ -ray intensities and assuming a 1.773 ± 0.003 sec half-life and a $(1.244 \pm 0.033)\%$ absolute intensity for the 1219-keV γ ray.

L. ^{38}Ca decay

As in previous studies^{68,69} of this decay, the ^{38}Ca activity was made by the reaction $^{36}\text{Ar}(^3\text{He}, n)^{38}\text{Ca}$. The ^{36}Ar gas was sealed in the rabbits by a soft self-sealing rubber plug (through which a hypodermic needle was inserted for evacuation and gas filling) and, at the beam entry end, by a $6.4\text{-}\mu\text{m}$ Ta foil. ^3He beams of 12 to 15 MeV entering the rabbit lost < 1.5 MeV in the Ta foil. A 0.25-mm-thick disc of Pt stopped the beam inside the rabbit.

The first part of the experiment measured the intensity of the 328-keV γ ray, emitted following β^+ decay to the 459-keV level of ^{38}K , relative to the intensity of the 1568-keV γ ray from the strong branch to the 1698-keV level. Positrons were stopped in a Lucite hutch and no Pb absorber was used. The difficulty in this measurement is the intense background near 328 keV produced principally by Compton scattering of 511-keV photons in the detector. This part of the experiment was performed in two separate runs. In the first, a 12.7-cm-diam by 10.2-cm-thick NaI(Tl) detector was used in a coincidence-anticoincidence arrangement to suppress the 511-keV Compton

TABLE IX. Relative intensities of daughter γ rays in $^{35}\text{Ar}(\beta + \gamma)^{35}\text{Cl}$.

E_γ^a (keV)	Transition ^a		This work ^b	Relative intensity		
	Initial state	Final state		c	d	e
916	3918	3003	f			
930	2694	1763	11.3 ± 2.6			
965	2968	3003	<8.7			
1219	1219		1000 ± 15	1000	1000	1000
1225	3918	2694	f			
1239	3003	1763	<3.0			
1274	3968	2694	<4.2			
1474	2694	1219	8.27 ± 1.27			
1763	1763		230.8 ± 3.7	234 ± 13	200 ± 27	180 ± 20
1783	3003	1219	<3.9			
1931	4624	2694	<2.1			
2155	3918	1763	<2.2			
2204	3968	1763	<2.7			
2645	2645		<1.2			e
2694	2694		109.6 ± 1.8		102 ± 15	e
2699	3918	1219	<3.3			
2748	3968	1219	4.80 ± 0.62			
2861	4624	1763	<0.99			
3003	3003		72.4 ± 1.4		90 ± 15	58 ± 15
3405	4624	1219	f			
3918	3918		5.21 ± 0.32			
3968	3968		1.06 ± 0.25			
4624	4624		<0.35			

^aLevel energies from Ref. 28.

^bUpper limits are 2σ confidence intervals (98% confidence).

^cReference 65.

^dReference 66.

^eReference 46. These authors did not report relative γ -ray intensities and they did not cite a reference for γ -ray branching in ^{35}Cl . They give an upper limit of 25 for the relative intensity of the 2645-keV branch and a relative intensity of 160 ± 20 for the 2694-keV branch.

^fPeak obscured by another peak.

background. Because the two 511-keV photons produced by annihilation of stopped positrons are emitted at 180° to each other, a second detector suitably placed on the opposite side of the source from the Ge(Li) detector is hit by a 511-keV photon whenever the Ge(Li) is hit, and vetoing these coincident events should eliminate much of the background. The system is not 100% efficient, of course, because of absorption, scattering, and the distributed source of annihilation radiation, such that the system reduced the background by a factor of only 1.7, and was not used in the second run. In analyzing the data from the first run, the possibility of a bias due to differences in the vetoing of the 328- and 1568-keV γ rays, because of the different energy distributions of the coincident positrons, was included in the uncertainty in the relative intensity. The relative-efficiency calibration was made with calibrated ^{133}Ba , ^{22}Na , and ^{60}Co sources and an uncalibrated ^{56}Co source. Corrections were made for absorption in the Ta and Al of the rabbit and also for the 0.51-mm Sn

and 0.25-mm Nb x-ray absorbers used in the second run. The spectra taken in the second run are shown in Figs. 13 and 14. The values of the intensity of the 328-keV γ ray, relative to the 1568-keV γ ray, were 0.116 ± 0.023 (first run) and 0.135 ± 0.021 (second run), with a weighted average of 0.126 ± 0.016 .

In the second part of the ^{38}Ca experiment, a 1.9-cm Pb absorber was used in a search for higher-energy γ rays. Table X summarizes the results of both relative intensity measurements, which are in reasonable agreement with previous results.^{68, 69}

We also measured the half-life by following the decay of the 1568-keV γ ray. Data were collected in 8 consecutive groups each lasting 0.26 sec. Four runs were made giving the following values for the ^{38}Ca half-life: 0.4099 ± 0.0175 sec, 0.4173 ± 0.0163 sec, 0.4596 ± 0.0183 sec, and 0.4375 ± 0.0163 sec. The weighted average is 0.430 ± 0.012 sec where the uncertainty has been increased because of the poor agreement of the four

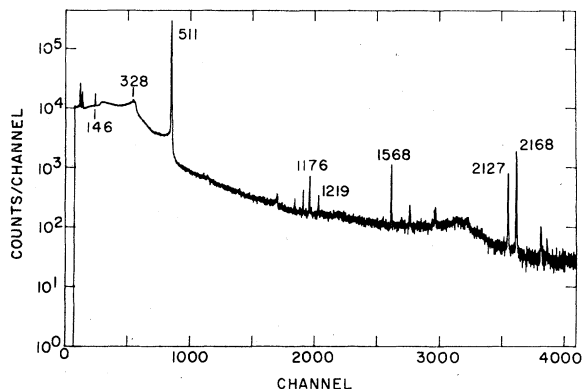


FIG. 13. The Ge(Li) spectrum taken in group 1 (0.00–0.45 sec) in the second run to measure the intensity of the 328-keV γ ray in ^{38}Ca decay. The only heavy absorber used was 0.51 mm of Sn, 0.25 mm of Nb, and 0.38 mm of Ta. The energy calibration is 0.598 keV/channel. All of the peaks have been identified except for a small peak at 349 keV. Prominent contaminant activities include $^{34}\text{Cl}^m$, ^{35}Ar , and ^{38}K , all produced in the ^{36}Ar target.

values. Gallmann *et al.*⁶⁹ report 0.439 ± 0.012 sec; the weighted average of their result and this work is 0.435 ± 0.009 sec which is adopted here in further calculations. We did not include the measurements of Kavanagh *et al.*⁶⁸ because of a known systematic error and of Zioni *et al.*⁷⁰ because of the large uncertainty.

Using the radiative corrections and Coulomb mixing given by Hardy and Towner³ and by Raman *et al.*⁴ and using the Q values for ^{38}Ca decay given by Endt and Van der Leun,²⁸ the partial half-life for the 0^+ to 0^+ superallowed Fermi transition to the 130-keV level of ^{38}K is calculated to be 0.5716 ± 0.0048 sec. Thus the branching ratio for the Fermi branch is 0.761 ± 0.017 .

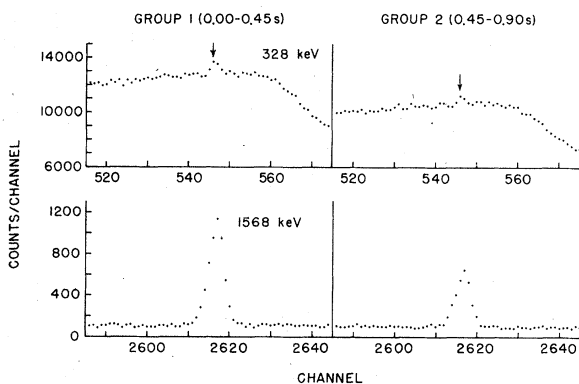


FIG. 14. Detailed spectra of the 328- and 1568-keV γ rays emitted in the decay of ^{38}Ca . The arrow indicates the position of the 328-keV γ ray calculated from the energy calibration. The group 1 data are the same as in Fig. 13.

Table I lists the absolute β -branch intensities and $\log ft$ values calculated from this work and Table II compares our results with several shell-model calculations of Gamow-Teller strengths.

M. ^{41}Sc decay

The ^{41}Sc activity was produced by the reaction $^{40}\text{Ca}(d,n)^{41}\text{Sc}$ in targets of natural Ca and 99.96% enriched ^{40}Ca , which were mounted in Be rabbits. The enriched ^{40}Ca targets were prepared by evaporation onto Pb target backings. The 6.0-MeV deuteron beam lost ~ 0.5 MeV in the beam-exit foil. In order to reduce oxidation and nitridation of gold-coated metallic targets, argon was used as the pusher gas.

The bombardment of ^{40}Ca by deuterons also produces ^{38}K and $^{38}\text{K}^m$. ^{38}K yields a 2167-keV γ ray in 99.9% of its decay so it was used as a monitor of the total number of $d + ^{40}\text{Ca}$ reactions and thus, of the total production of ^{41}Sc .

In the first part of the experiment, the intensity of the 2167-keV γ ray was measured relative to the total number of ^{41}Sc positrons. The targets were bombarded for 0.58 sec, a delay of 0.42 sec allowed the rabbits to travel to the detector, and then a counting period of 16 groups of 0.40 sec began. The cycle was repeated every 11.45 sec. The decay of the 511-keV peak was fitted with components with half-lives of 0.5963 sec (^{41}Sc), 0.9246 sec ($^{38}\text{K}^m$), and a long-lived component with a half-life between 64.6 sec (^{17}F) and 453 sec (^{38}K). One such run was done for each batch of targets (we used three batches in all) because the ratio of ^{38}K to ^{41}Sc production depends on the thickness of the targets used. Each run lasted 3435 sec (7.5 ^{38}K half-lives).

In the second part of the experiment, a 2.5-cm Pb absorber removed most of the 511-keV radiation. The beam was maintained at the same energy as in the first part to ensure the same relative production rates for ^{38}K and ^{41}Sc . The cycle used was similar to the cycle for the first part: beam on for 0.58 sec, a rabbit-transit delay of 0.42 sec, and a counting period of 2 groups of 0.80 sec repeated every 6.65 sec. Each run lasted 3438 sec (except for a few in which the target disintegrated or the rabbit broke). A typical spectrum obtained in this experiment is shown in Fig. 15. Detailed spectra are shown in Fig. 16. The high background above 5 MeV is due to the 6129-keV γ ray emitted in the decay of ^{16}N , produced in ^{15}N and ^{18}O contaminants in the targets. Relative-efficiency calibrations were made using ^{22}Na and ^{56}Co sources and the $^{14}\text{N}(p,\gamma)^{15}\text{O}$ reaction.

In the analysis of the data, it was necessary to take into account the contribution to the 2167-keV peak from the decay of ^{38}Cl produced in the

TABLE X. Relative intensities of γ rays in $^{38}\text{Ca}(\beta^+\gamma)^{38}\text{K}$.

E_γ ^a (keV)	Transition ^a		Relative intensities		
	Initial state	Final state	This work ^b	c	d
328	459	130	0.126 ± 0.016	<0.16	<0.14
1240	1698	459	<0.010	<0.04	<0.02
1568	1698	130	1	1	1
1643	3342	1698	<0.010		
1698	1698		<0.0082	<0.06	<0.02
1944	2402	459	<0.011	<0.16	
2646	2646		<0.0046		
2883	3342	459	<0.0033		
3185	3316	130	<0.0029		
3211	3342	130	0.0139 ± 0.0015		0.024 ± 0.008
3316	3316		<0.0027		
3342	3342		<0.0024		
3519	3978	459	<0.0042		
3710	3841	130	<0.0059		
3716	4175	459	<0.0045		
3726	3857	130	<0.0036		
3739	3739		<0.0036		
3848	3978	130	<0.0081		
4084	4214	130	<0.0029		
4318	4318		<0.0019		
4395	4395		<0.0037		

^aEnergies from Ref. 28.

^bUpper limits for this work are 2σ confidence intervals (98% confidence). Footnotes c and d do not state confidence levels for upper limits.

^cReference 68.

^dReference 69.

argon pusher gas. This contribution was determined from the observed 1642-keV γ ray from ^{38}Cl decay. Also, the decay of ^{49}Ca , produced in the small amount of ^{48}Ca in the targets, yielded a 3084-keV γ ray whose single-escape peak over-

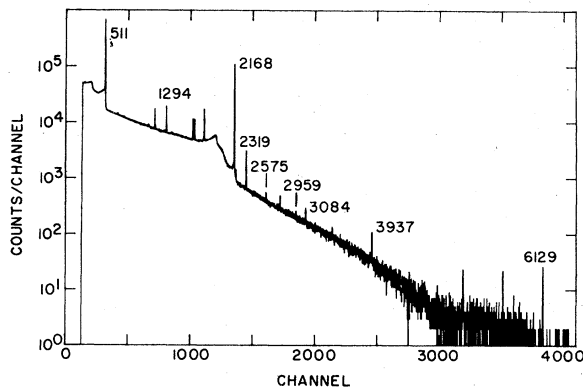


FIG. 15. A Ge(Li) spectrum taken in group 1 (0.00–0.8 sec) with one batch of enriched ^{40}Ca targets in the ^{41}Sc experiment. The energy calibration is 1.601 keV/channel. A 2.5-cm Pb absorber was used. All of the peaks have been identified except for a weak 672-keV γ ray with a half-life of ~ 0.8 sec. The 1294-, 2319-, 3084-, and 3937-keV peaks are due to ^{41}Ar , $^{90}\text{Zr}^m$, ^{49}Ca , and ^{38}K , respectively.

lapped the 2575-keV γ ray emitted in the decay of ^{41}Sc . Finally, the shorter cycle time in the second part increased the cycle efficiency for observing the 2167-keV γ ray from ^{38}K by a factor 1.72.

The results of this experiment are summarized in Table I. The half-life of 0.5963 ± 0.0017 sec is taken from Ref. 71. An upper limit of 1.7×10^{-5} is assigned for all branches to states above 4.5 MeV. The total intensity of all unobserved γ rays is $< 2.9 \times 10^{-4}$ of the ground-state branch which is a significant reduction from the limit $< 2 \times 10^{-3}$ given by Alburger and Wilkinson.

There is no reported shell-model calculation of Gamow-Teller strengths in the decay of ^{41}Sc , but rough estimates can be calculated from published spectroscopic factors²⁸ for the stripping reaction $^{40}\text{Ca}(d,p)^{41}\text{Ca}$. The spectroscopic factor S_n is the probability for the state structure, target nucleus (^{40}Ca) plus a neutron, with an orbital angular momentum determined by the angular distribution in the stripping reaction. Assuming that the ground state of ^{41}Sc is a $\frac{7}{2}^-$ proton coupled to a ^{40}Ca core, the Gamow-Teller matrix element for a transition to a $\frac{7}{2}^-$ state in ^{41}Ca is $|M_{GT}|^2 = \frac{9}{7}S_n$ and for a transition to a $\frac{5}{2}^-$ state $|M_{GT}|^2 = \frac{12}{7}S_n$. Because this model ignores the effect of polari-

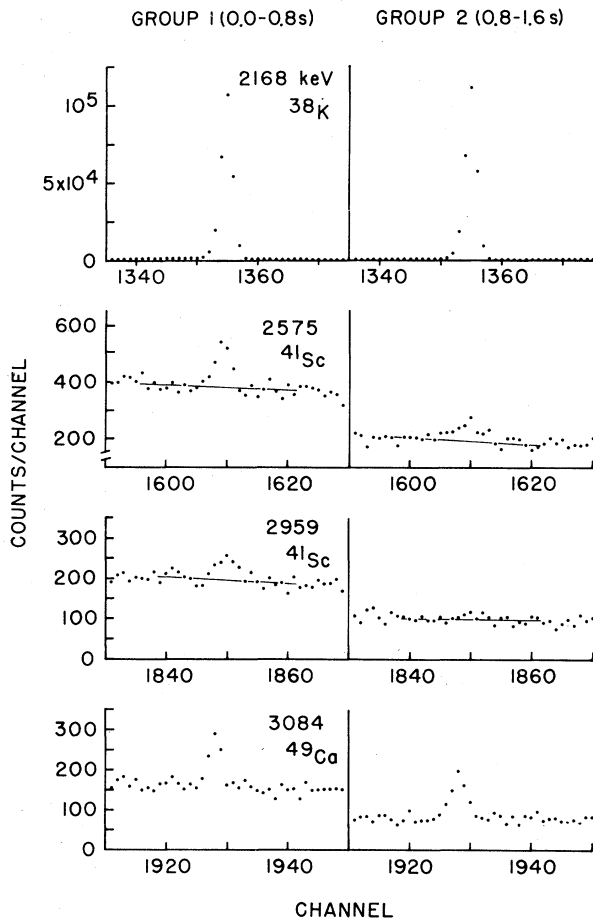


FIG. 16. Detailed spectra of the γ -ray peaks involved in calculating the intensities of the branches to the 2575- and 2959-keV levels in ^{41}Sc . The straight lines in the 2575- and 2959-keV plots are linear backgrounds. The group 1 data are the same as in Fig. 15.

zation of the ^{40}Ca core and because spectroscopic factors are not reliable to better than $\sim 20\%$, these estimates cannot be considered precise predictions of Gamow-Teller strengths. These estimates are shown in Table II. The high background in the 5- to 6-MeV region of the spectrum prevented testing even these estimates except for the 4878-keV state. We report new ^{41}Sc branches to the $\frac{5}{2}^-$ state at 2575 keV and the $\frac{1}{2}^-$ state at 2959 keV. Both of these are so weak that little can be said about the character of these states except that they have only a small single-particle component, in agreement with the $^{40}\text{Ca}(d, p)^{41}\text{Ca}$ results.

IV. CONCLUSIONS

This study has found 13 new Gamow-Teller branches in the decay of several intermediate mass nuclei and has improved the precision of the upper limits on the strengths of more than

50 others.

We do not discuss in detail the comparison between the measurements and the shell-model calculations shown in Table II. All of the calculations quoted used a large shell-model basis, with one exception,⁷² in which a closed ^{28}Si core was assumed in calculating $A = 38$ wave functions. Brown *et al.*¹ used a full $1s-0d$ shell basis and a 2-body interaction in which the matrix elements were adjusted to maximize agreement with observed excitation energies. Similarly, Timmer *et al.*⁷³ calculated transition strengths using wave functions calculated with an adjusted 2-body interaction and a basis for each A , J , and T consisting of up to 300 $1s-0d$ shell configurations expected to lie lowest in energy. Lanford and Wildenthal⁷⁴ report calculations of Gamow-Teller rates for most of the $1s-0d$ shell using different effective interactions and shell-model bases in different regions of the shell (in particular, they used a full $1s-0d$ shell basis for $A \leq 22$ and $A \geq 35$ and, for $A \geq 35$, a "realistic" interaction based on the Hamada-Johnston potential). The calculations of Glaudemans *et al.*⁷⁵ for $A = 30-34$ nuclei used wave functions that were similar to those used by Lanford and Wildenthal, with the similar results for predicted GT rates evident in Table II. Dieperink and Brussaard⁷⁶ calculated the 2-body interaction from the Tabakin potential and applied it to $A = 36$ to 39 nuclei using a full $1s-0d$ shell basis.

In most cases, the calculations correctly predict which transitions will be strong ($\log ft \leq 4$) and which will be weak ($\log ft \geq 5$); the stronger branches generally show better than factor-of-two accuracy in $|M_{\text{GT}}|^2$. A salient exception, not part of this work, is the ^{37}K decay to the 3171-keV $\frac{5}{2}^+$ state of ^{37}Ar , for which $\log ft > 6.3$ experimentally,³⁵ vs 3.91 theoretically.¹ For $A = 30$ the calculated and measured values show rather poor agreement for all branches.

Both Brown *et al.* and Lanford and Wildenthal are quite successful in calculating ^{21}Na decay in spite of the fact that this region of the $1s-0d$ shell is deformed. Similar agreement is found for ^{19}Ne and ^{23}Mg .

ACKNOWLEDGMENTS

We thank Dr. B. A. Brown, Dr. W. Chung, and Dr. B. H. Wildenthal for sending the results of their shell-model calculations prior to publication, and Barbara Cooper for assistance with the ^{31}S and ^{41}Sc experiments. We have profited from informative and stimulating discussions with Professor William A. Fowler. This work was supported in part by the National Science Foundation (PHY76-83685).

- *Present address: TRIUMF, University of British Columbia, Vancouver, B. C. V6T 2A3, Canada.
- †Present address: Hanford Engineering Development Laboratory, Richland, Washington 99352.
- ¹B. A. Brown, W. Chung, and B. H. Wildenthal, *Phys. Rev. Lett.* **40**, 1631 (1978) and private communication.
 - ²F. Meurders, P. W. M. Glaudemans, J. F. A. Van Hienen, and G. A. Timmer, *Z. Phys. A* **276**, 113 (1976).
 - ³J. C. Hardy and I. S. Towner, *Nucl. Phys.* **A254**, 221 (1975).
 - ⁴S. Raman, T. A. Walkiewicz, and H. Behrens, *At. Data Nucl. Data Tables* **16**, 451 (1975).
 - ⁵A. Kropf and H. Paul, *Z. Phys.* **267**, 129 (1974).
 - ⁶L. N. Bondarenko, V. V. Kurguzov, Yu. A. Prokof'ev, E. V. Rogov, and P. E. Spivak, *Pis'ma Zh. Eksp. Teor. Fiz.* **28**, 328 (1978) [*JETP Lett.* **28**, 303 (1978)].
 - ⁷A. Barroso and R. J. Blin-Stoyle, *Nucl. Phys.* **A251**, 446 (1975).
 - ⁸S. Raman, C. A. Houser, T. A. Walkiewicz, and I. S. Towner, *At. Data Nucl. Data Tables* **21**, 567 (1978).
 - ⁹N. B. Gove and M. J. Martin, *Nucl. Data Tables* **10**, 205 (1971).
 - ¹⁰I. S. Towner and F. C. Khanna, *Phys. Rev. Lett.* **42**, 51 (1979).
 - ¹¹D. H. Wilkinson, *Nucl. Phys.* **A209**, 470 (1973).
 - ¹²D. C. Camp and G. L. Meredith, *Nucl. Phys.* **A166**, 349 (1971).
 - ¹³G. J. McCallum and G. E. Coote, *Nucl. Instrum. Methods* **124**, 309 (1975).
 - ¹⁴R. A. Meyer, in *Table of Isotopes*, 7th ed., edited by C. M. Lederer and V. S. Shirley (Wiley, New York, 1978), Appendix II.
 - ¹⁵D. P. Donnelly, H. W. Baer, J. J. Reidy, and M. L. Wiedenbeck, *Nucl. Instrum. Methods* **57**, 219 (1967).
 - ¹⁶L. J. Jardine, *Phys. Rev. C* **11**, 1385 (1975).
 - ¹⁷M. R. Schmorak, *Nucl. Data Sheets* **22**, 487 (1977).
 - ¹⁸R. J. Gehrke, R. G. Helmer, and R. C. Greenwood, *Nucl. Instrum. Methods* **147**, 405 (1975).
 - ¹⁹U. Schötzig, K. Debertin, and K. F. Walz, *Int. J. Appl. Radiat. Isot.* **28**, 503 (1977).
 - ²⁰E. A. Henry, *Nucl. Data Sheets* **11**, 495 (1974).
 - ²¹R. L. Bunting, *Nucl. Data Sheets* **15**, 335 (1975).
 - ²²A. E. Evans, B. Brown, and J. B. Marion, *Phys. Rev.* **149**, 863 (1966).
 - ²³G. W. Grodstein, *NBS Circular* **583** (1957).
 - ²⁴G. Azuelos and J. E. Kitching, *At. Data Nucl. Data Tables* **17**, 103 (1976).
 - ²⁵A. T. Nelms, *NBS Circular* **577** (1956).
 - ²⁶R. M. Sternheimer, *Phys. Rev.* **103**, 511 (1956).
 - ²⁷H. W. Koch and J. W. Motz, *Rev. Mod. Phys.* **31**, 920 (1959).
 - ²⁸P. M. Endt and C. Van der Leun, *Nucl. Phys.* **A310**, 1 (1978).
 - ²⁹F. Ajzenberg-Selove, *Nucl. Phys.* **A268**, 1 (1976).
 - ³⁰R. W. Kavanagh and A. Knipper, *Bull. Am. Phys. Soc.* **10**, 715 (1965).
 - ³¹S. Cohen and D. Kurath, *Nucl. Phys.* **73**, 1 (1965).
 - ³²P. S. Hauge and S. Maripuu, *Phys. Rev. C* **8**, 1609 (1973).
 - ³³D. E. Alburger, *Phys. Rev. C* **9**, 991 (1974).
 - ³⁴G. Azuelos, J. E. Kitching, and K. Ramavataram, *Phys. Rev. C* **15**, 1847 (1977).
 - ³⁵F. M. Mann, H. S. Wilson, and R. W. Kavanagh, *Nucl. Phys.* **A258**, 341 (1976).
 - ³⁶L. Makela, P. B. Dworkin, and A. E. Litherland, *Bull. Am. Phys. Soc.* **14**, 550 (1969).
 - ³⁷T. T. Bardin, J. A. Becker, R. E. McDonald, and A. D. W. Jones, *Phys. Rev. C* **2**, 2283 (1970).
 - ³⁸F. Jundt, E. Aslanides, B. Fride, and A. Gallmann, *Nucl. Phys.* **A170**, 12 (1971).
 - ³⁹R. W. Kavanagh, *Nucl. Phys.* **A129**, 172 (1969) and unpublished results cited therein.
 - ⁴⁰C. E. Moss, C. Détraz, and C. S. Zaidins, *Nucl. Phys.* **A174**, 408 (1971).
 - ⁴¹J. C. Hardy, H. Schmeing, J. S. Geiger, and R. L. Graham, *Nucl. Phys.* **A246**, 61 (1975).
 - ⁴²H. Roderick, O. Lönsjö, and W. E. Meyerhof, *Phys. Rev.* **97**, 97 (1955).
 - ⁴³O. Lönsjö, *Phys. Norv.* **1**, 41 (1962).
 - ⁴⁴D. E. Alburger and D. R. Goosman, *Phys. Rev. C* **9**, 2236 (1974).
 - ⁴⁵J. Y. Gourlay, K. W. D. Ledingham, M. L. Fitzpatrick, and J. G. Lynch, *J. Phys. A* **6**, 415 (1973).
 - ⁴⁶C. Détraz, C. E. Moss, and C. S. Zaidins, *Phys. Lett.* **34B**, 128 (1971).
 - ⁴⁷W. L. Talbert and M. G. Stewart, *Phys. Rev.* **119**, 272 (1960).
 - ⁴⁸R. N. H. Haslam, R. G. Summers-Gill, and E. H. Crosby, *Can. J. Phys.* **30**, 257 (1952).
 - ⁴⁹M. V. Mihailović and B. Povh, *Nucl. Phys.* **7**, 296 (1958).
 - ⁵⁰J. Jänecke, *Z. Naturforsch.* **15A**, 593 (1960).
 - ⁵¹J. E. Cline and P. R. Chagnon, *Bull. Am. Phys. Soc.* **3**, 206 (1958).
 - ⁵²R. Wallace and J. A. Welch, *Phys. Rev.* **117**, 1297 (1960).
 - ⁵³P. J. Scanlon and D. Crabtree, *Can. J. Phys.* **48**, 1578 (1969).
 - ⁵⁴I. Tanihata, T. Minamisono, A. Mizobuchi, and K. Sugimoto, *J. Phys. Soc. Jpn.* **34**, 848 (1973).
 - ⁵⁵Th. Müller, E. S. Gelsema, and P. M. Endt, *Physica* **24**, 577 (1958).
 - ⁵⁶M. A. Van Driel, H. Klijnman, G. A. P. Engelbertink, H. H. Eggenhuisen, and J. A. J. Hermans, *Nucl. Phys.* **A240**, 98 (1975).
 - ⁵⁷D. H. White, R. E. Birkett, and T. Thomson, *Nucl. Instrum. Methods* **77**, 261 (1970).
 - ⁵⁸T. E. Ward and P. K. Kuroda, *J. Inorg. Nucl. Chem.* **33**, 609 (1971).
 - ⁵⁹I. M. Band, M. B. Trzhaskovskaya, and M. A. Listengarten, *At. Data Nucl. Data Tables* **18**, 433 (1976).
 - ⁶⁰E. L. Church and J. Weneser, *Annu. Rev. Nucl. Sci.* **10**, 193 (1960).
 - ⁶¹T. A. Green and M. E. Rose, *Phys. Rev.* **110**, 105 (1958).
 - ⁶²T. G. Ebrey and P. R. Gray, *Nucl. Phys.* **61**, 479 (1965).
 - ⁶³D. Green and J. R. Richardson, *Phys. Rev.* **101**, 776 (1956).
 - ⁶⁴H. S. Wilson and R. W. Kavanagh, *Bull. Am. Phys. Soc.* **21**, 1312 (1976).
 - ⁶⁵G. L. Wick, D. C. Robinson, and J. M. Freeman, *Nucl. Phys.* **A138**, 209 (1969).
 - ⁶⁶J. S. Geiger and B. W. Hooton, *Can. J. Phys.* **49**, 663 (1971).
 - ⁶⁷E. Hagberg, J. C. Hardy, B. Johnson, S. Mattsson, and P. Tidemand-Petersson, *Nucl. Phys.* **A313**, 276 (1979).
 - ⁶⁸R. W. Kavanagh, A. Gallmann, E. Aslanides, F. Jundt,

- and E. Jacobs, Phys. Rev. 175, 1426 (1968).
- ⁶⁹A. Gallmann, E. Aslanides, F. Jundt, and E. Jacobs, Phys. Rev. 186, 1160 (1969).
- ⁷⁰J. Zioni, A. A. Jaffe, E. Friedman, N. Haik, R. Schechtman, and D. Nir, Nucl. Phys. A181, 465 (1972).
- ⁷¹D. E. Alburger and D. H. Wilkinson, Phys. Rev. C 8, 657 (1973).
- ⁷²G. A. P. Engelbertink and P. W. M. Glaudemans, Nucl. Phys. A123, 225 (1969).
- ⁷³G. A. Timmer, F. Meurders, P. J. Brussaard, and J. F. A. Van Hienen, Z. Phys. A 288, 83 (1978).
- ⁷⁴W. A. Lanford and B. H. Wildenthal, Phys. Rev. C 7, 668 (1973).
- ⁷⁵P. W. M. Glaudemans, P. M. Endt, and A. E. L. Dieperink, Ann. Phys. (N.Y.) 63, 134 (1971).
- ⁷⁶A. E. L. Dieperink and P. J. Brussaard, Nucl. Phys. A128, 34 (1969).
- ⁷⁷E. L. Robinson and O. E. Johnson, Phys. Rev. 120, 1321 (1960).
- ⁷⁸G. Frick, A. Gallmann, D. E. Alburger, D. H. Wilkinson, and J. P. Coffin, Phys. Rev. 132, 2169 (1963).
- ⁷⁹D. C. Johnson, L. F. Chase, and W. L. Imhof, Bull. Am. Phys. Soc. 5, 406 (1960).
- ⁸⁰E. L. Robinson, J. I. Rhode, and O. E. Johnson, Phys. Rev. 122, 879 (1961).
- ⁸¹P. H. Barker, N. Drysdale, and W. R. Phillips, Proc. R. Phys. Soc. London 91, 587 (1967).
- ⁸²H. Schmeing, J. C. Hardy, R. L. Graham, and J. S. Geiger, Atomic Energy of Canada, Ltd. Report No. AECL-4078 (unpublished).
- ⁸³W. A. Hunt, R. M. Kline, and D. J. Zaffarano, Phys. Rev. 95, 611 (1954).
- ⁸⁴K. H. Lindenberger and J. A. Scheer, Z. Phys. 158, 111 (1960).
- ⁸⁵J. W. Nelson, E. B. Carter, G. E. Mitchell, and R. H. Davis, Phys. Rev. 129, 1723 (1963).
- ⁸⁶P. M. Endt and C. Van der Leun, Nucl. Phys. A214, 1 (1973).